Effect of interleukin 10 (IL-10) on liver fibrosis

Author: Messia Nazar
Student number: S4001079
Date: 8 April 2022
Supervisor: Prof. Dr. Klaas Poelstra
Department: Nanomedicine & Drug Targeting (NDT)

Table of content

Introduction

Chronic injury to the liver that causes inflammation can lead to liver fibrosis [1]. The source of injury varies from hepatitis B virus (HBV) or hepatitis C virus (HCV) to injury caused by excessive alcohol use and obesity [1]. The process from the start of the injury to a state of fibrosis may take up to around 30 years [1].
The hepatocytes are the parenchyma of the liver, which along with endothelial cells, Kupffer cells and hepatic stellate cells (HSC) make up the rest of the tissue [1]. Liver fibrosis affects the normal functioning of the liver by excessive accumulation of extracellular matrix (ECM) in the so called 'Space of Disse' by impairing blood supply from the hepatic portal vein to the hepatic parenchyma [1].

The ECM in a non-fibrotic liver is made up from collagen type IV, laminin and proteoglycans, whereas in a fibrotic liver the balance shifts more to collagen type I and III [2]. Those collagens are produced by activated HSC, which differentiate into ECM secreting myofibroblasts [2].

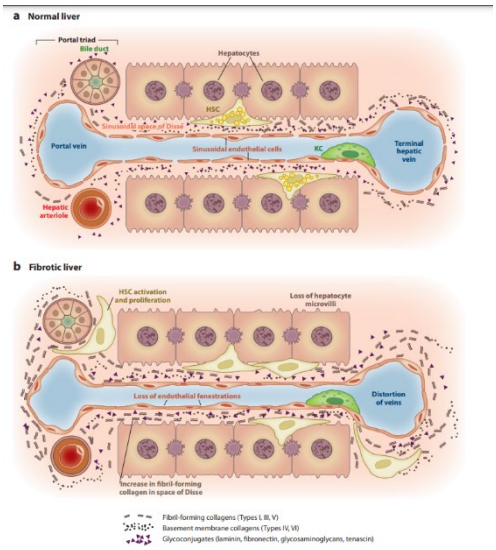

Figure 1. Difference between cellular composition and ECM deposition of (A) a normal liver and (B) a fibrotic liver [1].

The presence of a bacterial or viral toxin and subsequent activation of macrophages results in the release of multiple pro-inflammatory cytokines like tumor necrosis factor-a (TNF-a), IL-1, IL-6 and interferon-gamma (IFN-gamma) and leads to the increased expression of major histocompatibility complex-II (MHC-II) on the surface of M_1 macrophages [4-5]. Upon release of these cytokines, IL-10 is released to inhibit the inflammation [4-5]. This interleukin is seen as an anti-inflammatory cytokine that can possibly reverse the fibrotic state of the liver as IL-10 is expressed in various cells of the liver [3].
The IL-10 receptor is mainly present on the Kupffer cells as well on HSCs [4-5]. Some of the anti-inflammatory and anti-fibrotic effects of IL-10 reduce the production and secretion of the earlier mentioned cytokines by Kupffer cells [4-5]. Another effect is to inhibit the activation and differentiation of HSC into myofibroblasts as well as reducing the number of already activated HSCs [4-5].

On the contrary, some reports published provide evidence on the pro-inflammatory and pro-fibrotic effects of IL-10. Production of IFN-gamma and collagen were significantly increased as well as the inflammation in the portal area [6]. All of these effects resulted in an increase in liver fibrosis [6].

The question is therefore whether IL-10 is beneficial in the treatment of liver fibrosis. The aim of this project is to study the effect of IL-10 on some key parameters in this process. This will be determined by evaluating its effect on the nitric oxide (NO) production; on production of pro-inflammatory cytokines like IL-6 and TNF-a and the expression of MHC-II on M_1 macrophages. For the experiments RAW 264.7 cells will be used [7]. These are cells that resemble the macrophage cells/Kupffer cells and are functional and stable to use for experiments [7].

Materials and methods

Cell line

For all the experiments RAW 264.7 cells were used. They were cultured in heat inactivated Dulbecco's Modified Eagle Medium (DMEM supplemented with 10% fetal boval serum (FBS), gentamycin and pyruvate) at 37 °C and 5% CO_2. The first set of experiments had cells of passage 5 and the second set of experiments had cells of passage 8.

NO assay

For the determination of NO production by lipopolysaccharides (LPS), the RAW cells were first seeded in a 96-well plate for 24 hours. The supernatant was removed after 24 hours and fresh medium containing the correct concentration of LPS was added to the well, which was incubated for 24 hours. For determination of the effect of IL-10, the cells were pre-treated with 50 ng/mL IL-10 (the control samples were treated with DMEM) two hours prior to LPS addition. The NO assay was then conducted according to the NO assay protocol supplied in **Appendix C: figure 28**.

Determination gene expression IL-6, MHC-II and TNF-a by qPCR

The mRNA expressions of IL-6, MHC-II and TNF-a in response to LPS were determined using quantitative or real-time PCR. Here again the RAW 264.7 cells were first seeded in 24-well plate for 24 hours. After those 24 hours, the correct concentrations of LPS were added. Some of the well got a 50 ng/mL pre-treatment with IL-10 two hours prior to LPS addition, whereas the control samples were pre-treated with DMEM. One plate was incubated for just two hours upon LPS addition and another plate was incubated for 24 hours upon LPS addition. Before starting the RNA isolation, the samples were washed with phosphate buffered saline (PBS) before being stored at -80 °C. The mRNA expression levels of GAPDH (forward 5'-ACAGTCCATGCCATCACTGC-3' and reverse 5'-GATCCACGACGACATTG-3'), B-actin (forward 5'-ATCGTGCGTGACATCAAAGA-3' and reverse 5'-ATGCCACAGGATTCCATACC-3'), IL-6 (forward 5'-TGATGCTGGTGACAACCACGGC-3' and reverse 5'-TAAGCCTCCGACTTGTGAAGTGGTA-3'), MHC-II (forward 5'-TCCAGATGCCAACGTGGCCC-3' and reverse 5'-TGCGGAAGAGTGATCGTCCC-3') and TNF-a (forward 5'-CATCTTCTCAAAATTCGAGTGACAA-3' and reverse 5'-GAGTAGACAAGGTACAACCC-3') were determined according to the Maxwell® 16 LEV simplyRNA Cells Kit (see **Appendix C: figure 29-30** for the full protocol).

Immunohistochemical assessment fibrotic liver

For the immunohistochemical assessment of the fibrotic liver three markers were used: CD68 (marker for Kupffer cells), MHC-II (marker for M_1 macrophages) and collagen III (marker for ECM). The antigens used for these markers were rabbit anti-CD68 (for CD68; stock solution diluted 25 times), rat anti-MHC-II (for MHC-II; stock solution diluted 400 times) and goat anti-collagen III (for collagen III; stock solution diluted 100 times). The labelled antibodies (stock solutions diluted 50 times) used against these antigens were goat anti-rabbit (GARPO; against antigen for CD68), rabbit anti-rat (RARA; against antigen MHC-II) and rabbit anti-goat (RAGPO; against antigen for collagen III). For the staining of the liver sections the NovaRed® Substrate Kit was used. The whole procedure was conducted according to the protocol supplied in **Appendix C: figure 31**.

Statistical analysis

The results were processed using Excel and were expressed as mean ± SD. With T-tests the significance of the results were determined: $P < 0,05$ was considered as significant.

Results

Nitric oxide production of LPS stimulated RAW 264.7 cells

The effect of LPS on causing inflammation of RAW 264.7 cells was determined by the NO production. A NO assay was therefore performed. The RAW 264.7 cells stimulated with LPS showed a significant increase in NO production relative to the control ($P < 0,05$ for 0 ng/mL LPS vs. 100 ng/mL LPS), as shown in **figure 2** and. The negative control (NC) did not contain RAW 264.7 cells and were not stimulated with any concentration of LPS.

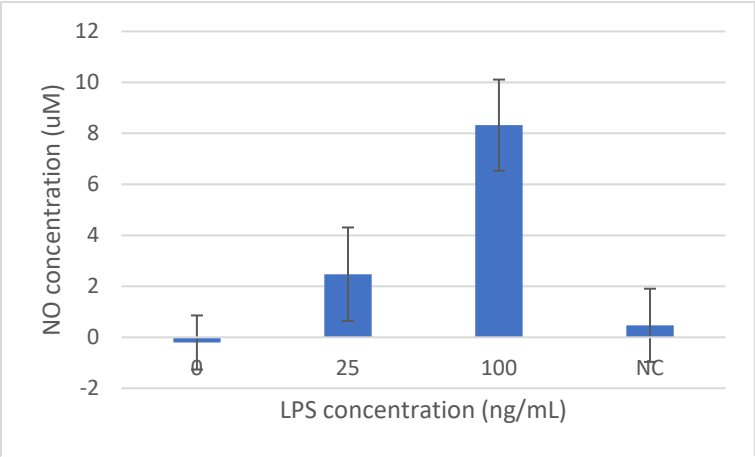

Figure 2. Effect of different concentrations LPS on NO production by RAW 264.7 cells (cell density of 1 x 10^5 cells/well)

Effect of cell density on nitric oxide production LPS induced RAW 264.7 cells

Three different cell densities (1 x 10^4 cells/well; 3 x 10^4 cells/well and 1 x 10^5 cells/well) of RAW 264.7 cells were stimulated with LPS to determine their NO production and see which cell density resulted in the highest response. The results of the NO assay along with microscopical imaging would give an indication on what the optimal cell density would be to use for the rest of the experiments. As seen in **figure 3**, there is an increase in NO production relative to the control for cell densities 3 x 10^4/well and 1 x 10^5/well (in both cases $P < 0,05$ for 0 ng/mL LPS vs 300 ng/mL LPS). There is, however, no significant increase in the NO production for the RAW 264.7 cells with a density of 1 x 10^4 cells/well.

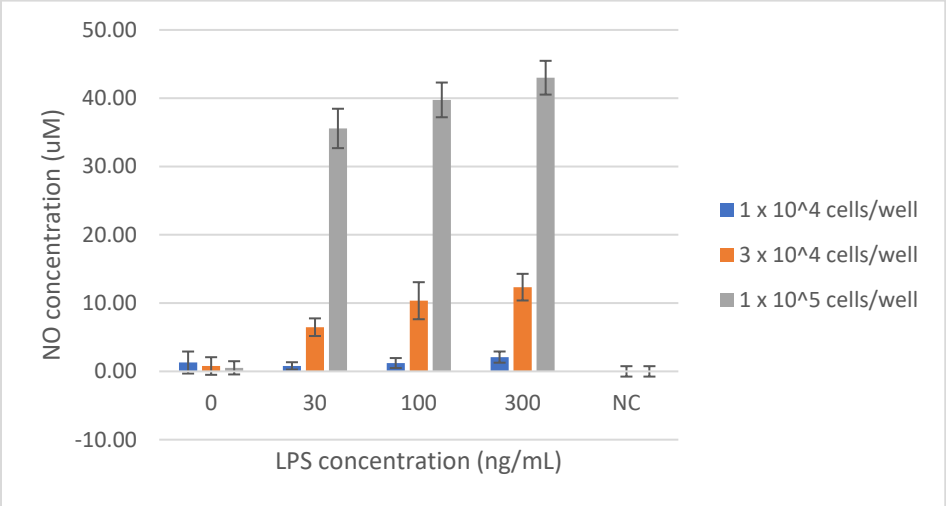

Figure 3. Effect of LPS concentrations and cell densities on the NO production by RAW 264.7 cells

Effect IL-10 on nitric oxide production LPS stimulated RAW 264.7 cells

As determined by earlier results, LPS was a potent inducer of NO production by RAW 264.7 cells. Therefore the effect of IL-10 on NO production was determined after LPS stimulation of RAW 264.7 cells. There is a significant increase in NO production relative to the control in all wells treated with LPS ($P < 0,05$ for 0 ng/mL LPS vs 300 ng/mL LPS). In the wells with IL-10 alone no significant ($P > 0,05$ for 0 ng/mL LPS vs 300 ng/mL LPS) NO response was found. However, the absolute concentrations of NO are much lower than what was measured in earlier experiments. In addition, there is no significant decrease in the NO production in pre-treated cells with 50 ng/mL IL-10 ($P > 0,05$).

In addition to the quantitative NO assay, microscopical images (**figures 5-8**) of the cells revealed a change in morphology after LPS stimulation both with and without pre-treatment of 50 ng/mL IL-10. As seen in the figures below, after every increasing LPS concentration, the morphology of the RAW 264.7 cells change from their known rounded-shape to a more spindle-shape. The same morphology change happened in the cells pre-treated with 50 ng/mL IL-10. There is no difference seen between the cells treated with IL-10 and the cells not treated with IL-10 cells: they show the same amount of round- and spindle-shaped RAW 264.7 cells. It therefore appears that the cells do respond to LPS despite the low NO production found in **figure 4**.

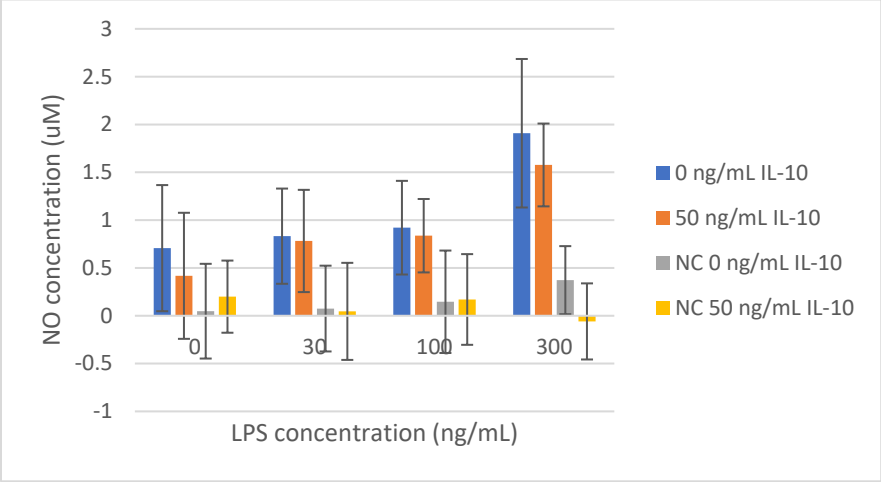

Figure 4. Effect LPS concentration on NO production by RAW 264.7 cells (cell density of 3 x 10^4 cells/well). In addition, the effect of IL-10 on the NO production of RAW 264.7 cells for different LPS concentrations

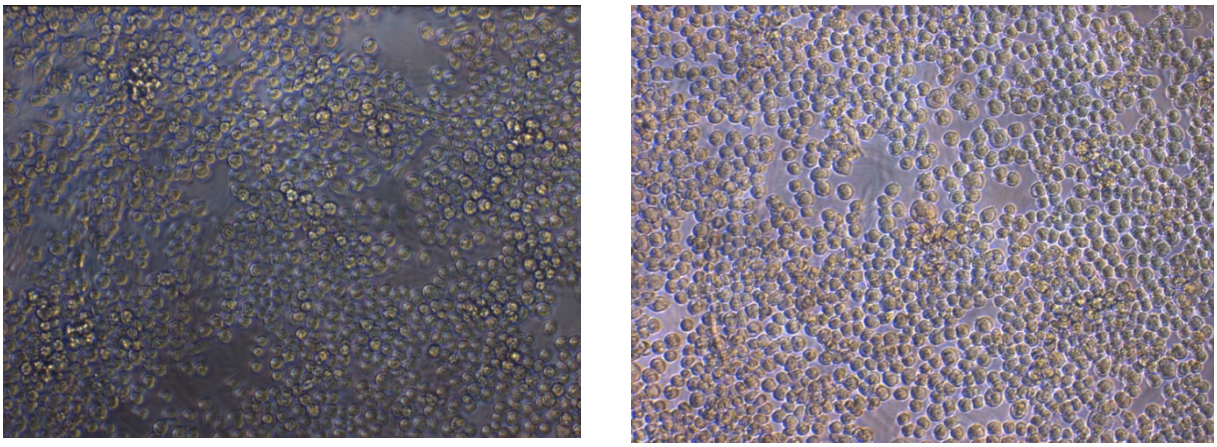

Figure 5. Microscopical image of RAW 264.7 cells with 0 ng/mL LPS stimulation and no IL-10 pre-treatment (left) and with 50 ng/mL IL-10 pre-treatment (right)

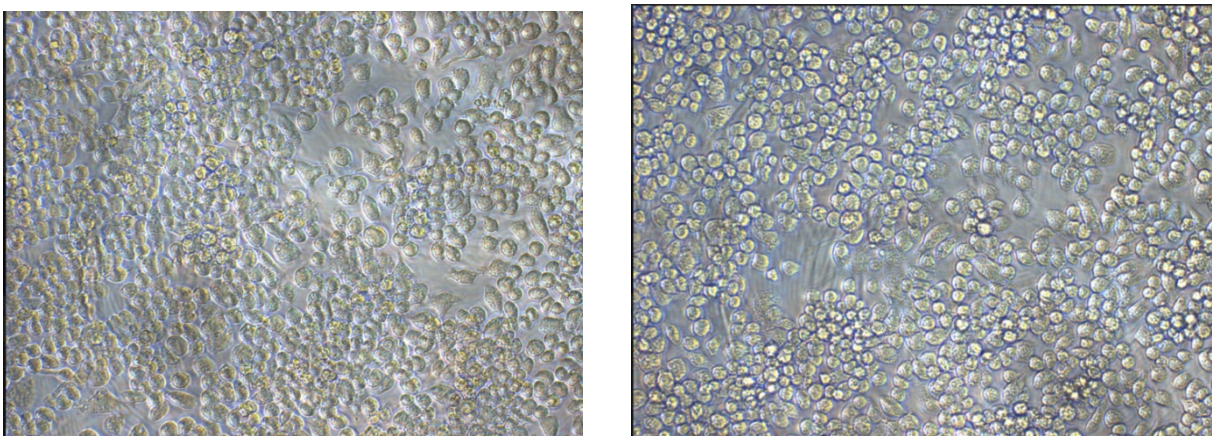

Figure 6. Microscopical image of RAW 264.7 cells with 30 ng/mL LPS stimulation and no IL-10 pre-treatment (left) and with 50 ng/mL IL-10 pre-treatment (right)

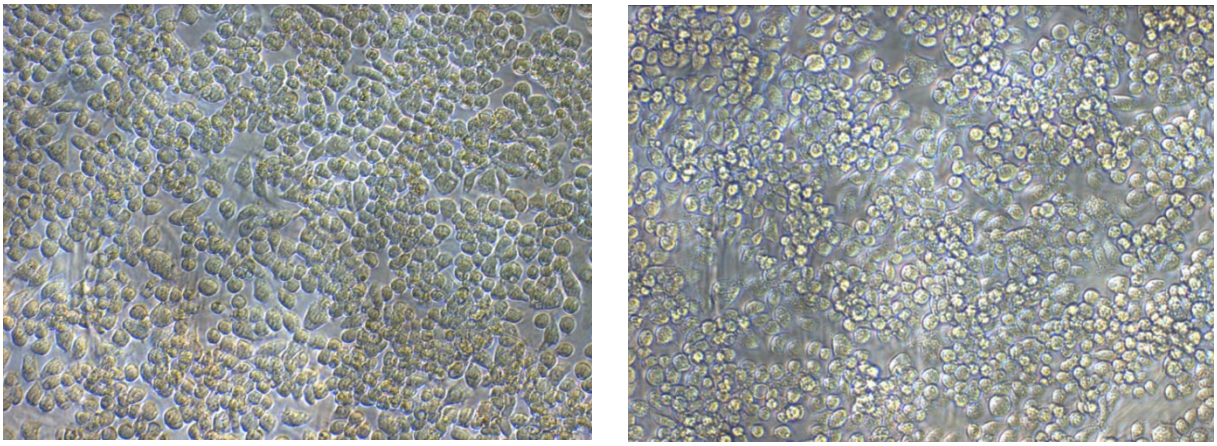

Figure 7. Microscopical image of RAW 264.7 cells with 100 ng/mL LPS stimulation and no IL-10 pre-treatment (left) and with 50 ng/mL IL-10 pre-treatment (right)

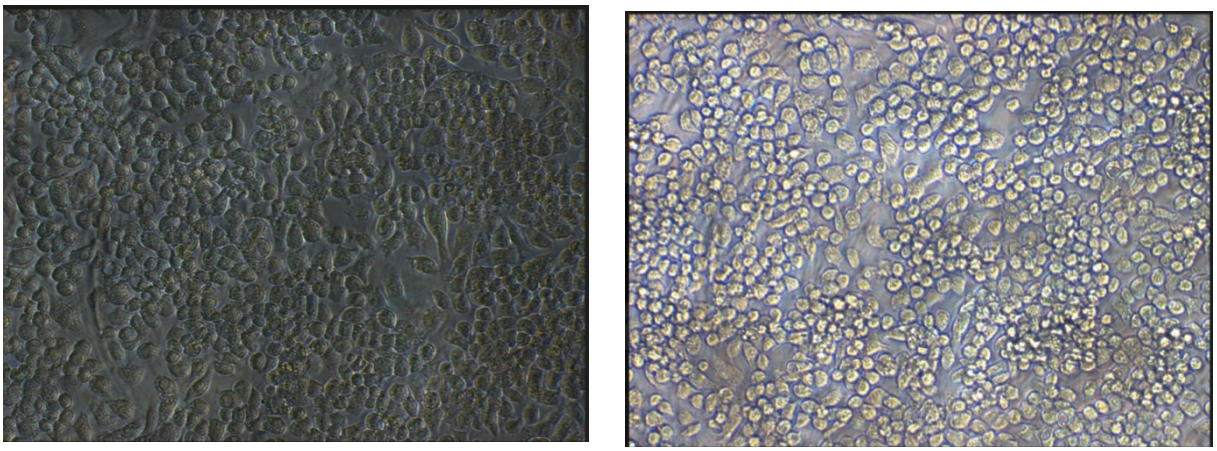

Figure 8. Microscopical image of RAW 264.7 cells with 300 ng/mL LPS stimulation and no IL-10 pre-treatment (left) and with 50 ng/mL IL-10 pre-treatment (right)

Effects IL-10 on gene expression IL-6, MHC-II and TNF-a

Real-time or quantitative PCR was used to determine the expression of IL-6, MHC-II and TNF-a after LPS stimulation of RAW 264.7 cells. One set of cells were stimulated with LPS for two hours, whereas another set of cells were stimulated for 24 hours. In addition, the effect of IL-10 on the same set of gene expression in the RAW 264.7 cells was determined. As seen in **figure 9**, LPS increased the IL-6 expression significantly but only after 24 hours ($P < 0,05$ for 0 ng/mL LPS vs. 300 ng/mL LPS). Just like that, IL-10 caused a significant reduction of the IL-6 gene expression ($P < 0,05$) as the relative gene expression reduced by almost 2-fold.

The same result is seen for the gene expression of MHC-II, where there is a significant increase after 24 hours ($P < 0,05$ for 0 ng/mL LPS vs 300 ng/mL LPS) but not after two hours. However, the absolute gene expression of MHC-II was higher after two hours than after 24 hours. As opposed to IL-6, there is no significant reduction of MHC-II gene expression after two nor 24 hours LPS stimulation of pre-treated RAW 264.7 cells with IL-10 ($P > 0,05$ for 0 ng/mL LPS vs 300 ng/mL LPS).

The TNF-a gene expression did not significantly increase or decrease after two hours nor after 24 hours of LPS stimulation ($P > 0,05$ for 0 ng/mL LPS vs 300 ng/mL LPS). Pre-treatment of IL-10 also did not have a significant effect on the TNF-a expression in the RAW 264.7 cells.

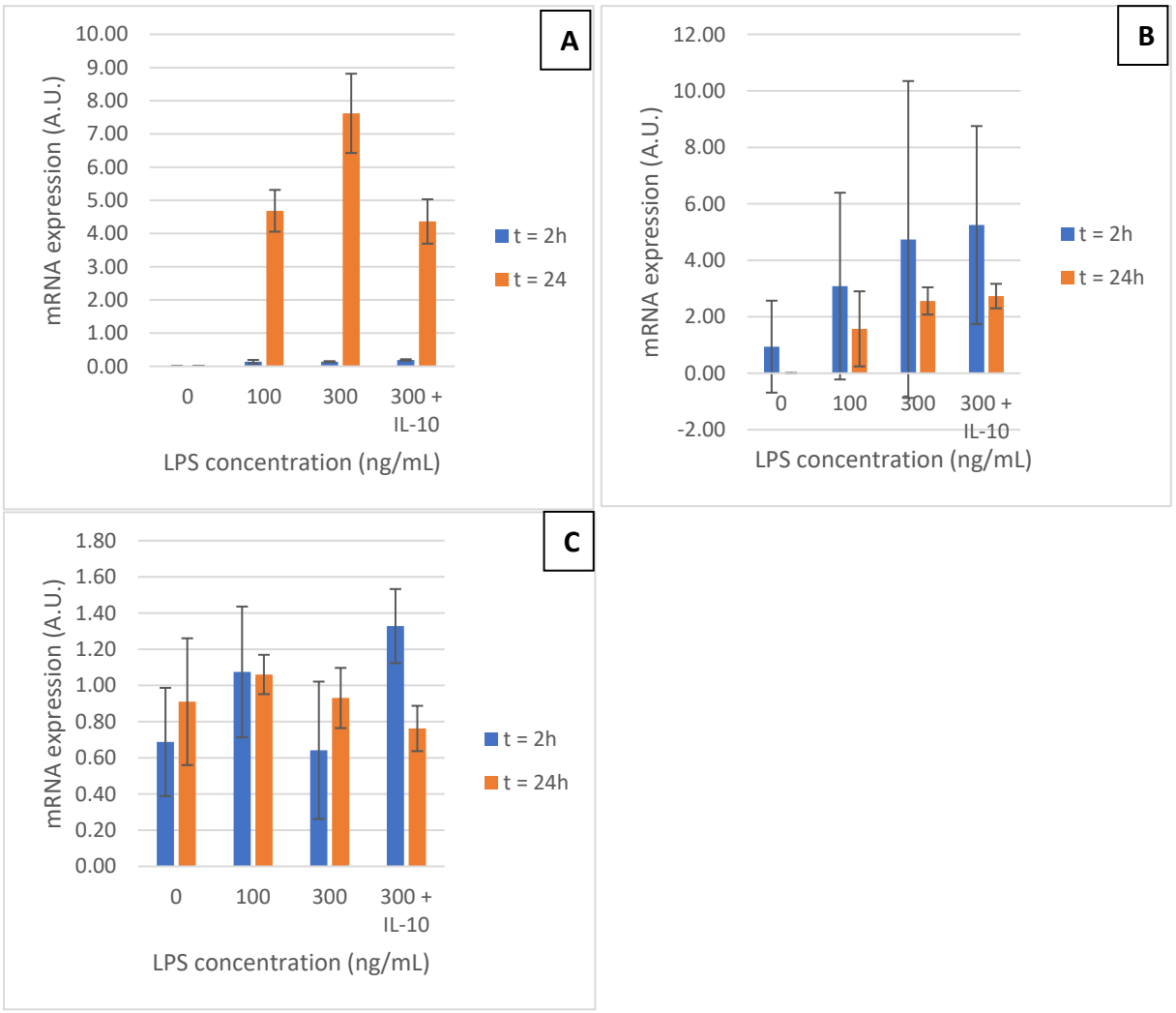

Figure 9. Effect LPS concentrations and IL-10 pre-treatment (50 ng/mL) on (A) IL-6 mRNA expression; (B) MHC-II mRNA expression and (C) TNF-a mRNA expression

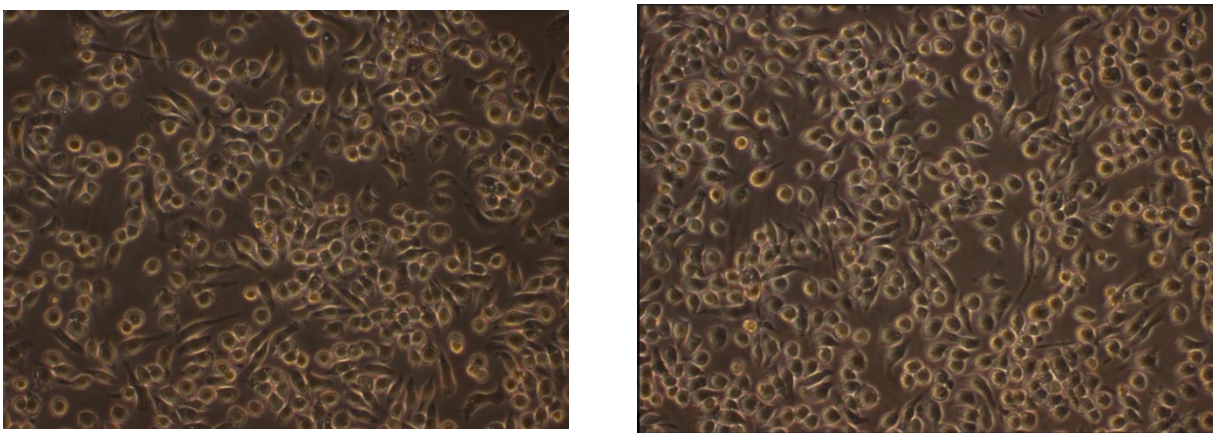

Figure 10. Microscopical image of RAW 264.7 cells before LPS stimulation and no IL-10 pre-treatment (left) and 50 ng/mL IL-10 pre-treatment. The images show no difference of cell morphology and amount of cells.

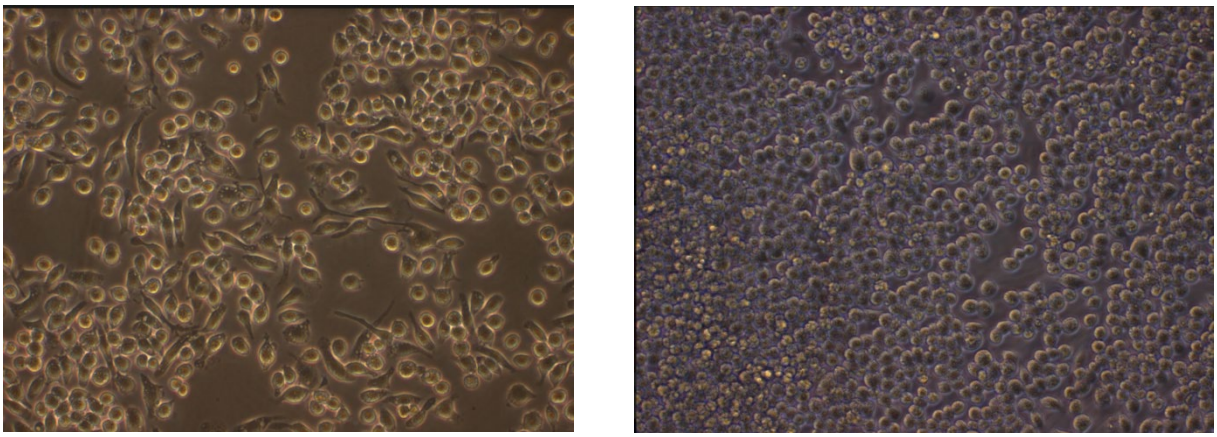

Figure 11. Microscopical image of RAW 264.7 cells after 2 hours (left) and 24 hours (right) after 0 ng/mL LPS stimulation. The images show a difference in amount of cells; i.e. there are more cells after 24 hours than after two hours.

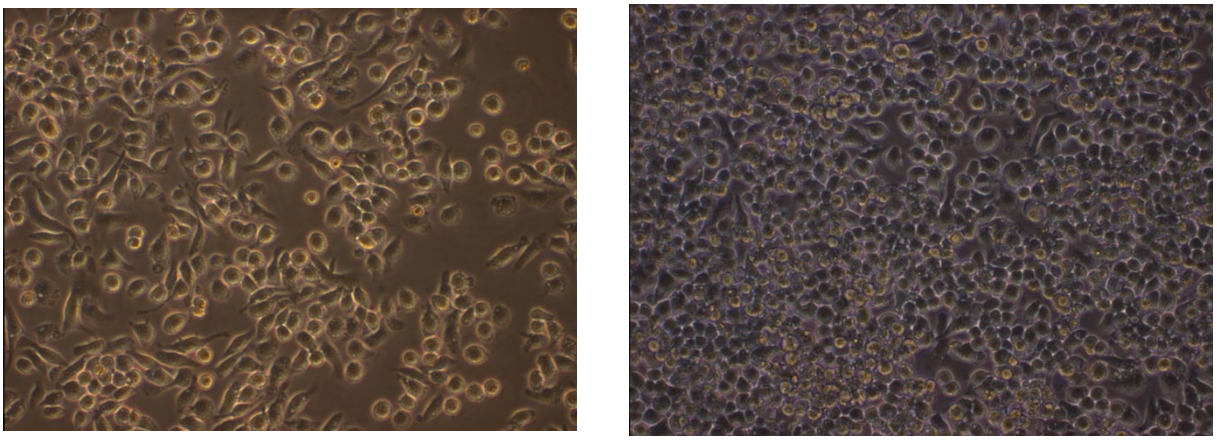

Figure 12. Microscopical image of RAW 264.7 cells after 2 hours (left) and 24 hours (right) after 100 ng/mL LPS stimulation. This figure again shows more cells after 24 hours of LPS stimulation compared to two hours of LPS stimulation. There is no difference in the morphology of the cells between two and 24 hours LPS stimulation.

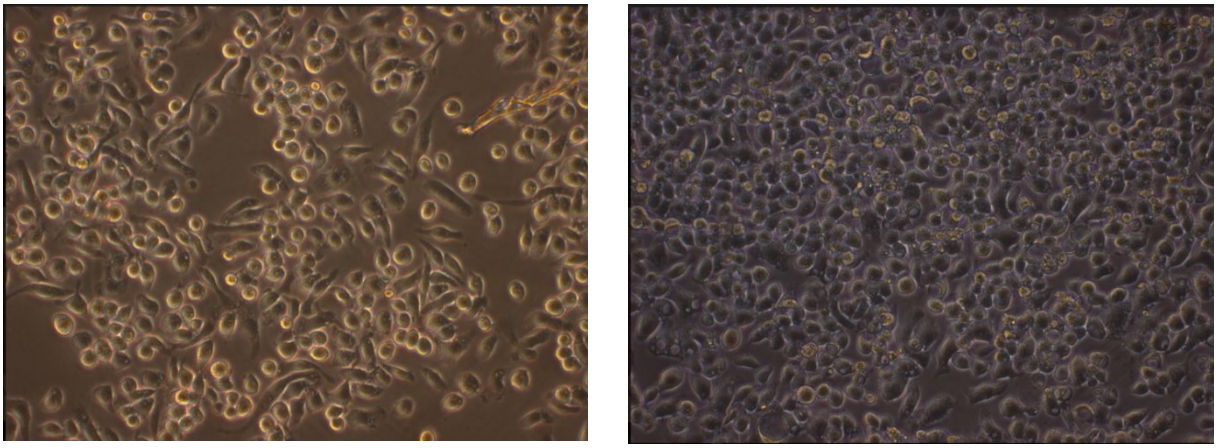

Figure 13. Microscopical image of RAW 264.7 cells after 2 hours (left) and 24 hours (right) after 300 ng/mL LPS stimulation. The images show the again a difference in cell amount between two hours LPS stimulation and 24 hours LPS stimulation. At this LPS concentration there is clearly a difference seen in the morphology after 24 hours LPS stimulation.

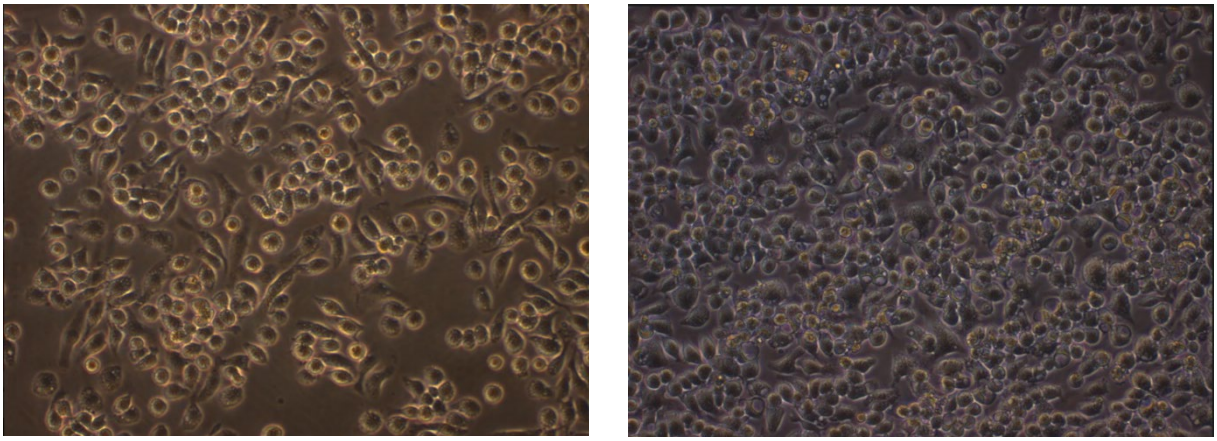

Figure 14. Microscopical image of RAW 264.7 cells after 2 hours (left) and 24 hours (right) after 300 ng/mL LPS stimulation and 50 ng/mL IL-10 pre-treatment. The images show no effect of IL-10 pre-treatment on the cell morphology and cell amount after two hours of LPS stimulation and after 24 hours of LPS stimulation.

As seen in **figures 10-14**, microscopical images also show the effect of LPS stimulation and IL-10 pre-treatment on the morphology of the RAW 264.7 cells. First, it is visible that after 24 hours of seeding, the cells have slightly changed their morphology; i.e. more spindle-shaped cells are formed. There is no difference in the cells pre-treated with 50 ng/mL IL-10 and those that do not have seen IL-10. Another observation is that higher concentrations of LPS increased the amount of those spindle-shaped cells after both two and 24 hours. There is not much of a difference between the IL-10 untreated and IL-10 treated RAW 264.7 cells. Another difference is the cell density after two and 24 hours: the cell density is significantly higher after 24 hours than after two hours.

Immunohistochemical assessment fibrotic liver

The following images show the histology of healthy liver tissues compared to fibrotic livers. The three proteins on the liver cells that are stained immunohistochemically are collagen III, CD68 and MHC-II.

In **figure 16** the collagen III is stained on the liver slices. The collagen III expression is visible on the hepatic portal vein and is significantly increased in the fibrotic liver section compared to the healthy liver section.

The CD68 is usually present on the Kupffer cells of the liver. As the Kupffer cells line the

endothelial cells from the hepatic portal vein to the hepatic artery, there is a clear staining present in those areas. In the fibrotic liver section there is an increase in the CD68 expression compared to the healthy liver section. The increase is especially visible in the area around the hepatic artery as depicted by the arrows in **figure 17**.
As MHC-II are present on antigen-presenting cells (APCs) they will be present on M_1 macrophages, which will be present in the whole inflamed area of the liver tissue. Comparing the healthy and the fibrotic liver section, in **figure 18,** there is an increase in MHC-II expression in the diseased liver section compared to the healthy liver section.

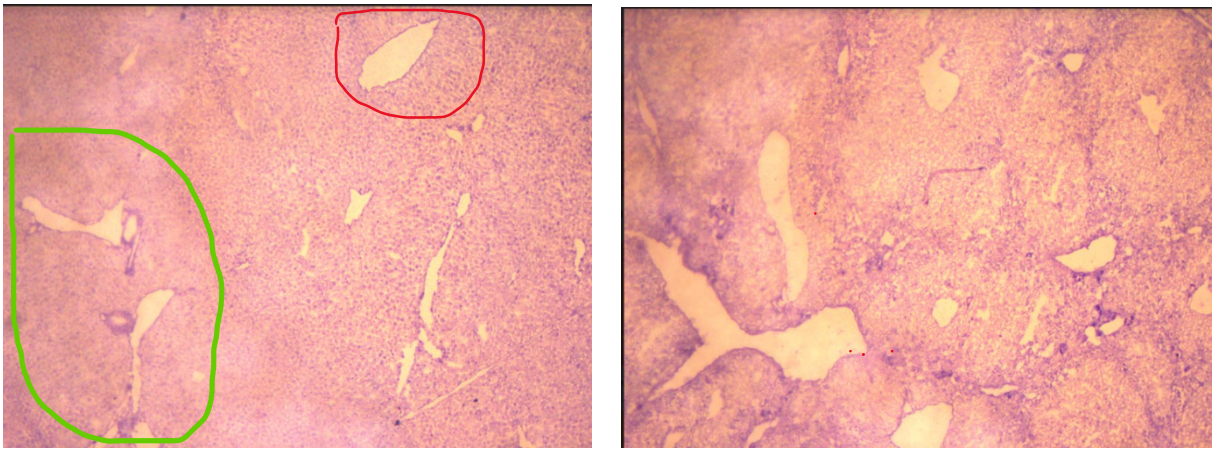

Figure 15. Immunohistochemical staining for 'healthy' (left; green marks the portal area while red marks the hepatic artery) and 'fibrotic' (right) liver section.

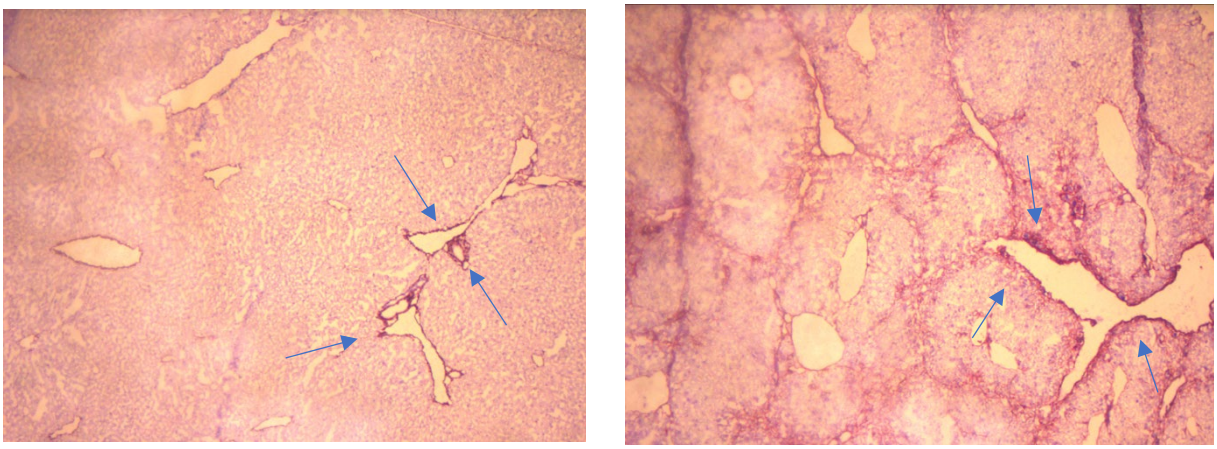

Figure 16. Immunohistochemical staining of collagen III in a 'healthy' (left) and a 'fibrotic' (right) liver section

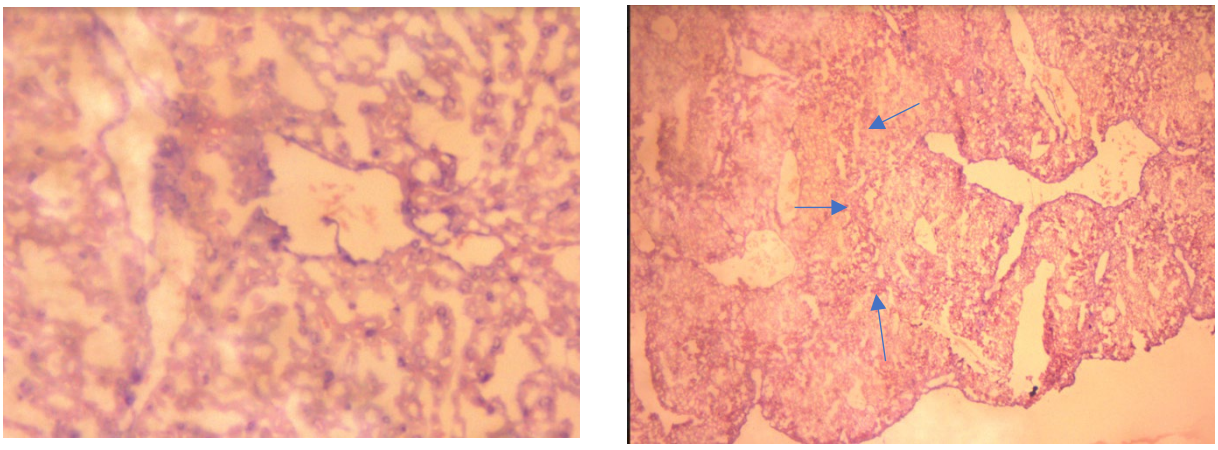

Figure 17. Immunohistochemical staining of CD^{68} in a 'healthy' (left) and a 'fibrotic' (right) liver section

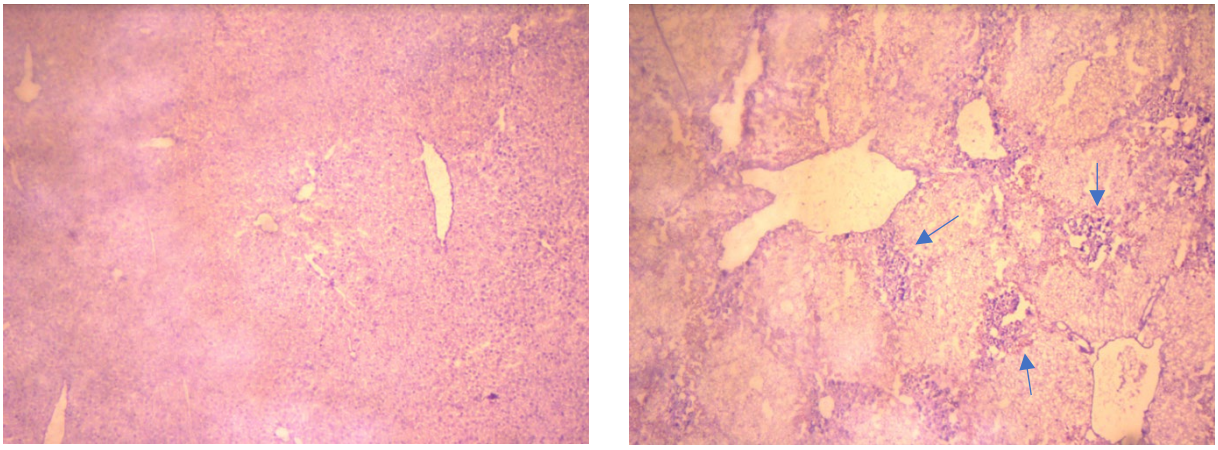

Figure 18. Immunohistochemical staining of MHC-II in a 'healthy (left) and a 'fibrotic' (right) liver section

Discussion

NO production LPS stimulated RAW 264.7 cells

The stimulation of NO production from the RAW 264.7 cells was induced by LPS, which is part of the cell wall of gram-negative bacteria [8]. As gram-negative bacteria have an inner and outer membrane, the LPS is attached to the bilayer of the outer membrane [8]. LPS consists of three distinctive parts: lipid A, the core oligosaccharide and an antigen O [8]. It is the lipid A that causes the endotoxic effect of LPS by binding to Toll-Like-receptor 4 (TLR_4) [8]. Especially the LPS derived from *E.Coli* are very potent in causing immunological reactions [8].

As seen in the results, higher concentrations of LPS caused more NO production, which was determined by an NO assay. For the binding of LPS to TLR_4, three elements are necessary: LPS binding protein (LBP), CD14 and MD2 [9-10]. The TLR_4, amongst others present on the RAW 264.7 cells, activates Myeloid Differentiation 88 primary response (MyD88-) and TIR-domain-containing adaptor-inducing interferon-b (TRIF-) dependent pathway [9-10]. On their turn these pathways lead to the activation of nuclear factor kappa-light-chain-enhancer of activated B cells (NF-kB) and mitogen-activated protein kinase (MAPK), which are responsible for the regulation of the transcription of inducible nitric oxide synthase (iNOS) and release of many pro-inflammatory cytokines [9-10]. Some of those cytokines also upregulate the iNOS expression [9-10].

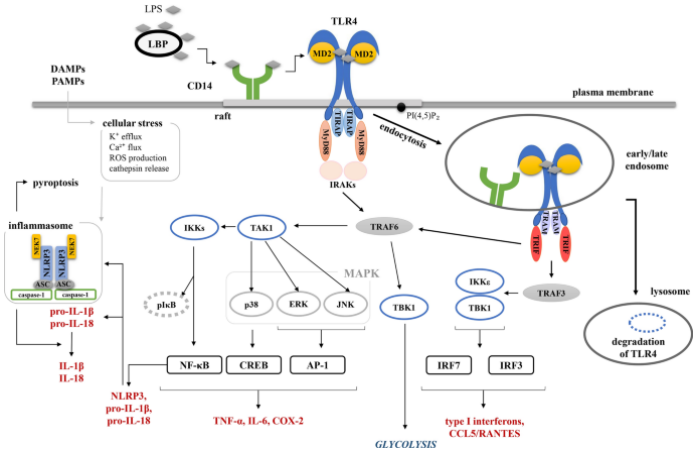

Figure 19. MyD88-dependent and TRIF-dependent signalling pathway of TLR_4 upon activation by LPS [10]

This is also what was seen in the NO assays, as higher concentrations of LPS caused significantly increased ($P < 0,05$) NO production by the RAW 264.7 cells.

Effect cell density on NO production

The absolute concentration of NO production was also determined by the cell density of the wells. As seen in **figure 3**, higher the cell densities caused more NO production. As there was no significant increase in the NO production by LPS stimulation for a cell density of 1 x 10^4 cells/well, this cell density was deemed inappropriate. As already said, a combination of the NO production and microscopical imaging would indicate the best cell density. As both cell densities of 3 x 10^4 cells/well and 1 x 10^5 cells/well caused a significant increase in NO production the microscopic images gave the breakthrough in the choice for a cell density of 3 x 10^4 cells/well. Due to the fact that RAW 264.7 cells needed more space upon LPS stimulation was a reason to go with a cell density of 3 x 10^4 cells/well as in that case more space was available in the well.

Effect IL-10 on NO production

The anti-inflammatory and anti-fibrotic effect of IL-10 was measured with the stimulation of the RAW 264.7 cells with different concentrations of LPS. As seen in **figure 4**, pre-treatment of the RAW 264.7 cells with 50 ng/mL IL-10 did not reduce the NO production significantly. IL-10 is known to reduce the activation of NF-kB and MAPK, which are under normal circumstances activated by TLR_4 [11-12]. This reduced activity of NF-kB and MAPK is due to the fact of reduced MyD88 protein expression in the RAW 264.7 cells [11-12]. The MyD88-independent (TRIF-dependent) pathway does not play a role in the reduced activity of NF-kB and MAPK [11-12]. In addition, IL-10 also induces the SOCS-3 expression in RAW 264.7 cells upon activation of the IL-10R [11-12]. An effect of this induced SOCS-3 expression is a decrease in iNOS expression and subsequent NO production [11-12].

The fact that the NO production of pre-treated RAW 264.7 cells was not significantly reduced relative to untreated RAW 264.7 cells might be more due to the fact that there was not even a stable baseline NO production by the RAW 264.7 cells to begin with. This low NO response is not caused by any problem with LPS used and the possible higher passage number of the RAW 264.7 cells, as the same results were obtained with newly produced LPS and RAW 264.7 cells with a lower passage number (**figure 20: Appendix A**). Also it was unlikely that the passage number of the RAW 264.7 cells were at fault for the low NO response, as the passage number of the cells used were 5 and 8 and the functional stability of those cells are high up until passage numbers above 30 [13]. The Griess reagent necessary for the NO assay was also changed, and also did not induce the NO response to LPS, as seen in **figure 20**.

Another theory for this low NO response might be the sudden shut off of iNOS expression in the RAW 264.7 cells. This can be proven by quantitatively determining the iNOS mRNA expression by qPCR.

Effect IL-10 gene expression IL-6, MHC-II and TNF-a

As earlier explained for the NO production, activation of the TLR_4 by LPS activates the MyD88-dependent and TRIF-dependent signalling pathways. Those two pathways activate NF-kB and MAPK, which amongst others cause the production of pro-inflammatory cytokines like IL-6 and TNF-a. In addition, LPS stimulated RAW 264.7 cells become M_1 macrophages and increase their MHC-II expression. As seen in **figure 9**, there is indeed a significant increase in the IL-6 and MHC-II expression after 24 hours of LPS stimulation. There is, in contrast to the theory [4-5], no significant increase in the TNF-a mRNA expression after two hours nor after 24 hours of LPS stimulation (**figure 9**). As this is not in line with the theory, the qPCR of TNF-a has to be run again for confirmation.
Earlier described was the effect of IL-10 on the reduction of NO production by the RAW 264.7 cells. The same theory is valid for the production of pro-inflammatory cytokines like IL-

6 and TNF-a. However, it is only the IL-6 mRNA expression that is significantly reduced after IL-10 pre-treatment; TNF-a mRNA expression did not significantly decrease upon IL-10 treatment. As IL-10 induces the alternative macrophage activation (M_2) instead of the classical macrophage activation, there will be less MHC-II mRNA expression as M_2 does not express MHC-II. This is again not confirmed by the data obtained, as there is no decrease, let alone a significant one, of the MHC-II mRNA expression after both two hours and 24 hours.

To check for the quality of the qPCR, two household genes in GAPDH and b-actin were chosen, as seen in **figure 24**. Both genes did not show an increase or decrease in mRNA expression upon LPS concentrations. In addition, stable and consistent standard, amplification and melt curves were obtained for both genes, which further indicated their viability as household genes.
Similarly, the standard curve for IL-6 is provided with an R^2 of 0,96 and an efficiency% of ± 121%, which are acceptable values. The amplification and melt curves show no outliers, which also confirm that the samples were pure. The standard curves for MHC-II and TNF-a, however, have an R^2 of 0,128 and 0,886; respectively. In addition, their efficiencies are far above 100%, which are unacceptable values and indicate that the results are not useful. Their amplification and melt curves show that the samples were pure, except for the melt curve for MHC-II which have multiple curves with more peaks indicating impurities. Therefore the results of the qPCR for MHC-II and TNF-a are not useful and should be performed again for confirmation.

Immunohistochemical assessment fibrotic liver

In all of the fibrotic liver sections there are clear signs of fibrosis visible. One of the elements to recognize fibrosis in immunohistochemistry is the deposition of ECM in the parenchymal cells of the liver [14]. Whereas in a healthy liver the ECM is mainly composed of collagen type IV, in a fibrotic liver the balance shifts more to collagen type I and III [14]. Collagen type III is, in fibrotic liver, mainly localized in the wall of the blood vessels and around the portal areas [14]. This is also seen in **figures 16**, where the staining of collagen type III is increased in the hepatic portal vein of the fibrotic liver section compared to the healthy liver section. The production of ECM is controlled by quiescent HSC (qHSC) which transform into ECM producing myofibroblasts upon activation by inflammatory stimuli [15].

Another element of liver fibrosis is the involvement of tissue resident macrophages of the liver, Kupffer cells [16]. In response to LPS, the Kupffer cells activate and differentiate into M_1 macrophages to secrete pro-inflammatory cytokines like IL-6 and TNF-a, as already mentioned earlier. One of the markers for Kupffer cells is CD68 [17]. As seen in **figure 17**, there is an increased CD68 expression in the fibrotic liver compared to the healthy liver. As those Kupffer cells are located near the endothelial cells, which go from the portal vein to the hepatic artery, especially those areas are stained.

In addition to CD68 there is another marker for M_1 macrophages: MHC-II. As more Kupffer cells will be activated and differentiated into M_1 macrophages, more expression of MHC-II will be present in the fibrotic liver sections compared to healthy liver sections. This is also seen in **figure 18**, where there is increased MHC-II stained in the fibrotic liver section in the same area as the CD68.

Conclusion

From the results it can be concluded that LPS stimulation of RAW 264.7 cells causes, in most of the cases, a NO response. In addition to the NO production, there is also a significant increase in mRNA expression of IL-6. The effect of LPS on the mRNA expression of MHC-II and TNF-a were unreliable and those experiments should be performed again.
It was also seen that IL-10 did not have an effect on the NO production by those RAW 264.7 cells upon LPS stimulation. However, it did significantly decrease the IL-6 mRNA expression. As the results of the qPCR for MHC-II and TNF-a were unreliable no conclusion can be drawn on those parameters.
Due to the varying results regarding the effect of IL-10 on inflammatory cytokines, no conclusion can be drawn yet on whether IL-10 might be beneficial as treatment for liver fibrosis.

As the NO production by the RAW 264.7 cells upon LPS stimulation was not consistent, further studies can be focused on the expression of iNOS upon LPS stimulation. Furthermore, the presence and expression of the IL-10 receptor on various liver cells can be determined, which can be valuable for further studies on the effects of IL-10.

References

[1]. *Hernandez-Gea, V., & Friedman, S. L. (2011). Pathogenesis of liver fibrosis. Annual review of pathology, 6, 425–456.* https://doi.org/10.1146/annurev-pathol-011110-130246

[2]. *Gressner A. M. (1996). Transdifferentiation of hepatic stellate cells (Ito cells) to myofibroblasts: a key event in hepatic fibrogenesis. Kidney international. Supplement, 54, S39–S45.*

[3]. *An, S. Y., Petrescu, A. D., & DeMorrow, S. (2021). Targeting Certain Interleukins as Novel Treatment Options for Liver Fibrosis. Frontiers in pharmacology, 12, 645703.* https://doi.org/10.3389/fphar.2021.645703

[4]. *de Waal Malefyt, R., Abrams, J., Bennett, B., Figdor, C. G., & de Vries, J. E. (1991). Interleukin 10(IL-10) inhibits cytokine synthesis by human monocytes: an autoregulatory role of IL-10 produced by monocytes. The Journal of experimental medicine, 174(5), 1209–1220.* https://doi.org/10.1084/jem.174.5.1209

[5]. *de Waal Malefyt, R., Haanen, J., Spits, H., Roncarolo, M. G., te Velde, A., Figdor, C., Johnson, K., Kastelein, R., Yssel, H., & de Vries, J. E. (1991). Interleukin 10 (IL-10) and viral IL-10 strongly reduce antigen-specific human T cell proliferation by diminishing the antigen-presenting capacity of monocytes via downregulation of class II major histocompatibility complex expression. The Journal of experimental medicine, 174(4), 915–924.* https://doi.org/10.1084/jem.174.4.915

[6]. *Hsueh, Y. H., Chen, H. W., Syu, B. J., Lin, C. I., Leung, P., Gershwin, M. E., & Chuang, Y. H. (2018). Endogenous IL-10 maintains immune tolerance but IL-10 gene transfer exacerbates autoimmune cholangitis. Journal of autoimmunity, 95, 159–170.* https://doi.org/10.1016/j.jaut.2018.09.009

[7]. *Taciak, B., Białasek, M., Braniewska, A., Sas, Z., Sawicka, P., Kiraga, Ł., Rygiel, T., & Król, M. (2018). Evaluation of phenotypic and functional stability of RAW 264.7 cell line through serial passages. PloS one, 13(6), e0198943.* https://doi.org/10.1371/journal.pone.0198943

[8]. *Bertani, B., & Ruiz, N. (2018). Function and Biogenesis of Lipopolysaccharides. EcoSal Plus, 8(1), 10.1128/ecosalplus.ESP-0001-2018.* https://doi.org/10.1128/ecosalplus.ESP-0001-2018

[9]. *Deng, S., Yu, K., Zhang, B., Yao, Y., Wang, Z., Zhang, J., Zhang, X., Liu, G., Li, N., Liu, Y., & Lian, Z. (2015). Toll-Like Receptor 4 Promotes NO Synthesis by Upregulating GCHI Expression under Oxidative Stress Conditions in Sheep Monocytes/Macrophages. Oxidative medicine and cellular longevity, 2015, 359315.* https://doi.org/10.1155/2015/359315

[10]. *Ciesielska, A., Matyjek, M., & Kwiatkowska, K. (2021). TLR4 and CD14 trafficking and its influence on LPS-induced pro-inflammatory signaling. Cellular and molecular life sciences : CMLS, 78(4), 1233–1261.* https://doi.org/10.1007/s00018-020-03656-y

[11]. *Dagvadorj, J., Naiki, Y., Tumurkhuu, G., Hassan, F., Islam, S., Koide, N., Mori, I., Yoshida, T., & Yokochi, T. (2008). Interleukin-10 inhibits tumor necrosis factor-alpha production in lipopolysaccharide-stimulated RAW 264.7 cells through reduced MyD88 expression. Innate immunity, 14(2), 109–115.* https://doi.org/10.1177/1753425908089618

[12]. *Berlato, C., Cassatella, M. A., Kinjyo, I., Gatto, L., Yoshimura, A., & Bazzoni, F. (2002). Involvement of suppressor of cytokine signaling-3 as a mediator of the inhibitory effects of IL-*

10 on lipopolysaccharide-induced macrophage activation. Journal of immunology (Baltimore, Md. : 1950), 168(12), 6404–6411. https://doi.org/10.4049/jimmunol.168.12.6404

[13]. *Taciak, B., Białasek, M., Braniewska, A., Sas, Z., Sawicka, P., Kiraga, Ł., Rygiel, T., & Król, M. (2018). Evaluation of phenotypic and functional stability of RAW 264.7 cell line through serial passages. PloS one, 13(6), e0198943. https://doi.org/10.1371/journal.pone.0198943*

[14]. *u, W. D., Zhang, Y. E., Zhai, W. R., & Zhou, X. M. (1999). Dynamic changes of type I,III and IV collagen synthesis and distribution of collagen-producing cells in carbon tetrachloride-induced rat liver fibrosis. World journal of gastroenterology, 5(5), 397–403. https://doi.org/10.3748/wjg.v5.i5.397*

[15]. *Aydın, M. M., & Akçalı, K. C. (2018). Liver fibrosis. The Turkish journal of gastroenterology : the official journal of Turkish Society of Gastroenterology, 29(1), 14–21. https://doi.org/10.5152/tjg.2018.17330*

[16]. *Slevin, E., Baiocchi, L., Wu, N., Ekser, B., Sato, K., Lin, E., Ceci, L., Chen, L., Lorenzo, S. R., Xu, W., Kyritsi, K., Meadows, V., Zhou, T., Kundu, D., Han, Y., Kennedy, L., Glaser, S., Francis, H., Alpini, G., & Meng, F. (2020). Kupffer Cells: Inflammation Pathways and Cell-Cell Interactions in Alcohol-Associated Liver Disease. The American journal of pathology, 190(11), 2185–2193. https://doi.org/10.1016/j.ajpath.2020.08.014*

[17]. *Wikipedia contributors. (2021, July 5). Wikipedia. Retrieved April 6, 2022, from https://en.wikipedia.org/wiki/CD68*

Appendix

Appendix A. NO assays of LPS stimulated RAW 264.7 cells

*Table 1. Data NO assay corresponding to **figure 2***

LPS concentration (ng/mL)	***Absorbance***								
	1	**2**	**3**	**4**	**5**	**6**	**7**	**8**	**9**
0	0,056	0,065	0,061	0,059	0,056	0,054	0,051	0,056	0,056
25	0,078	0,071	0,088	0,09	0,078	0,066	0,121	0,1	0,063
100	0,14	0,132	0,14	0,152	0,148	0,153	0,145	0,14	0,117
NC	0,059	0,062	0,06	0,099	0,246	0,057	0,057	0,059	0,056
LPS concentration (ng/mL)	***Concentration (uM)***								
	1	**2**	**3**	**4**	**5**	**6**	**7**	**8**	**9**
0	0,58	1,65	1,18	-0,53	-0,81	-1,00	-1,28	-0,81	-0,81
25	3,20	2,37	4,39	2,40	1,26	0,13	5,32	3,34	-0,15
100	10,58	9,63	10,58	8,25	7,87	8,34	7,58	7,11	4,94
NC	0,94	1,30	1,06	3,25	17,11	-0,72	-0,72	-0,53	-0,81
LPS concentration (ng/mL)	***Average concentration (uM) ± SD***								
0	-0,20 ± *1,06*								
25	2,47 ± *1,83*								
100	8,32 ± *1,79*								
NC	0,47 ± *1,43*								

*Table 2. Data NO assay corresponding to **figure 3** (cell density: 1 x 10^4 cells/well)*

LPS concentration (ng/mL)	***Absorbance***			***Concentration (uM)***			***Average concentration (uM) ± SD***
	1	**2**	**3**	**4**	**5**	**6**	
0	0,09	0,09	0,07	1,86	2,55	-0,52	1,30 ± *1,61*
30	0,08	0,08	0,08	1,41	0,61	0,39	0,80 ± *0,54*
100	0,09	0,08	0,09	1,52	0,39	1,75	1,22 ± *0,73*
300	0,10	0,08	0,09	2,77	1,18	2,32	2,09 ± *0,82*

*Table 3. Data NO assay corresponding to **figure 3** (cell density: 3 x 10^4 cells/well)*

LPS concentration (ng/mL)	***Absorbance***								
	1	**2**	**3**	**4**	**5**	**6**	**7**	**8**	**9**
0	0,08	0,07	0,08	0,07	0,09	0,08	0,07	0,07	0,07
30	0,13	0,13	0,13	0,12	0,11	0,12	0,11	0,14	0,12
100	0,16	0,17	0,18	0,11	0,13	0,14	0,18	0,18	0,15
300	0,18	0,39	0,15	0,14	0,18	0,17	0,18	0,18	0,20
NC	0,06	0,42	0,07	0,06	0,07	0,07	0,07	0,07	0,07
LPS concentration (ng/mL)	***Concentration (uM)***								
	1	**2**	**3**	**4**	**5**	**6**	**7**	**8**	**9**
0	1,54	-0,30	0,84	0,74	3,34	1,80	-0,52	-0,64	0,27
30	7,99	7,46	8,12	6,06	5,35	6,18	4,82	7,32	4,93
100	12,07	12,59	13,64	5,23	7,95	8,66	11,86	11,75	9,36
300	14,83	41,28	10,09	9,13	13,51	12,09	12,55	12,20	14,25
NC	-0,96	45,22	-0,43	-0,09	0,50	0,97			
LPS concentration (ng/mL)	***Average concentration (uM) ± SD***								
0	0,79 ± *1,29*								
30	6,47 ± *1,29*								
100	10,35 ± *2,71*								
300	12,33 ± *1,95*								
NC	0,00 ± *0,76*								

*Table 4. Data NO assay corresponding to **figure 3** (cell density: 1 x 10^5 cells/well)*

LPS concentration (ng/mL)	***Absorbance***					
	1	**2**	**3**	**4**	**5**	**6**
0	0,07	0,07	0,07	0,07	0,07	0,08
30	0,34	0,38	0,35	0,35	0,34	0,38
100	0,39	0,39	0,38	0,37	0,39	0,40
300	0,42	0,63	0,38	0,41	0,41	0,46
	0,06	0,42	0,07	0,06	0,07	0,07
LPS concentration (ng/mL)	***Concentration (uM)***						***Average concentration (uM) ± SD***
	1	**2**	**3**	**4**	**5**	**6**	
0	-0,30	0,36	-0,57	0,86	0,62	2,16	0,52 ± *0,97*
30	34,70	40,09	36,14	33,26	32,08	37,16	35,57 ± *2,88*
100	42,33	42,20	40,49	35,74	37,99	39,77	39,75 ± *2,54*
300	45,62	72,99	40,75	40,83	41,42	46,39	43,00 ± *2,47*
NC	-0,96	45,22	-0,43	-0,09	0,50	0,97	0,00 ± *0,76*

*Table 5. Data NO assay corresponding to **figure 4** (0 ng/mL IL-10)*

LPS concentration (ng/mL)	***Absorbance***								
	1	**2**	**3**	**4**	**5**	**6**	**7**	**8**	**9**
0	0,067	0,066	0,066	0,061	0,061	0,065	0,062	0,058	0,058
30	0,067	0,066	0,066	0,061	0,063	0,063	0,064	0,06	0,062
100	0,069	0,063	0,067	0,064	0,062	0,063	0,067	0,061	0,062
300	0,081	0,071	0,073	0,069	0,070	0,066	0,082	0,067	0,07
LPS concentration (ng/mL)	***Concentration (uM)***								
	1	**2**	**3**	**4**	**5**	**6**	**7**	**8**	**9**
0	1,51	1,39	1,39	0,54	0,54	1,01	0,37	-0,20	-0,20
30	1,51	1,39	1,39	0,54	0,78	0,78	0,65	0,08	0,37
100	1,73	1,06	1,51	0,90	0,66	0,78	1,07	0,23	0,37
300	3,08	1,96	2,18	1,48	1,60	1,13	3,18	1,07	1,49
LPS concentration (ng/mL)	***Average concentration (uM) ± SD***								
0	0,71 ± *0,66*								
30	0,83 ± *0,50*								
100	0,92 ± *0,49*								
300	1,91 ± *0,78*								

*Table 6. Data NO assay corresponding to **figure 4** (pre-treatment with 50 ng/mL IL-10)*

LPS concentration (ng/mL)	***Absorbance***								
	1	**2**	**3**	**4**	**5**	**6**	**7**	**8**	**9**
0	0,062	0,064	0,063	0,059	0,062	0,063	0,055	0,057	0,058
30	0,064	0,063	0,064	0,065	0,064	0,063	0,058	0,068	0,059
100	0,064	0,066	0,065	0,064	0,063	0,063	0,062	0,062	0,063
300	0,067	0,068	0,067	0,065	0,065	0,068	0,076	0,073	0,073
LPS concentration (ng/mL)	***Concentration (uM)***								
	1	**2**	**3**	**4**	**5**	**6**	**7**	**8**	**9**
0	0,94	1,17	1,06	0,31	0,66	0,78	-0,62	-0,34	-0,20
30	1,17	1,06	1,17	1,01	0,90	0,78	-0,20	1,21	-0,06
100	1,17	1,39	1,28	0,90	0,78	0,78	0,37	0,37	0,51
300	1,51	1,62	1,51	1,01	1,01	1,37	2,34	1,92	1,92
LPS concentration (ng/mL)	***Average concentration (uM) ± SD***								
0	0,42 ± *0,66*								
30	0,78 ± *0,53*								
100	0,84 ± *0,38*								
300	1,58 ± *0,43*								

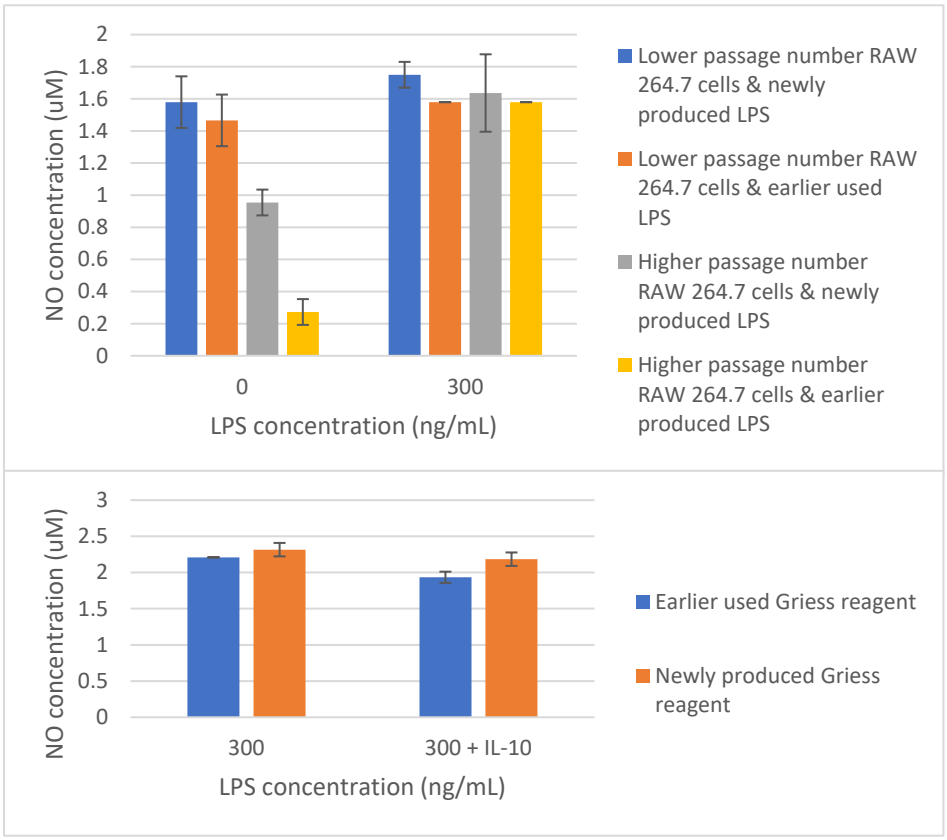

Figure 20. Effect passage number, LPS and Griess reagent on NO production by RAW 264.7 cells

Appendix B. Effect IL-10 on gene expression IL-6, MHC-II and TNF-a

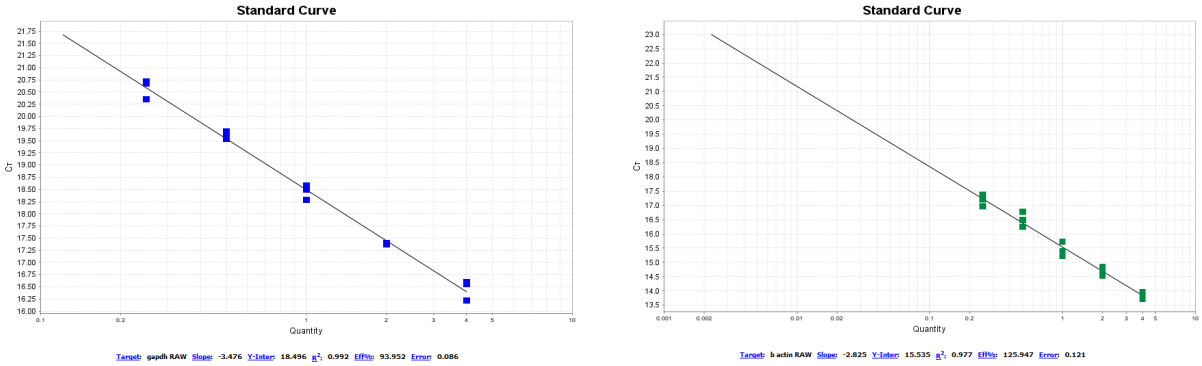

Figure 21. Standard curves of GAPDH (y = -3,476x + 18,496) with an R^2 of 0,992 and an efficiency% of 93,952% (left) and of b-actin (y = -2,825x + 15,535) with an R^2 of 0,977 and an efficiency% of 125,947% (right)

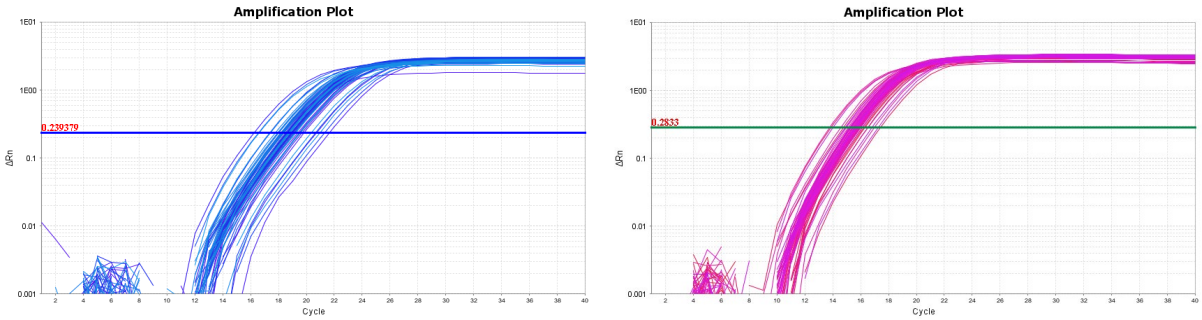

Figure 22. Amplification plots of the qPCR of GAPDH (left) and b-actin (right)

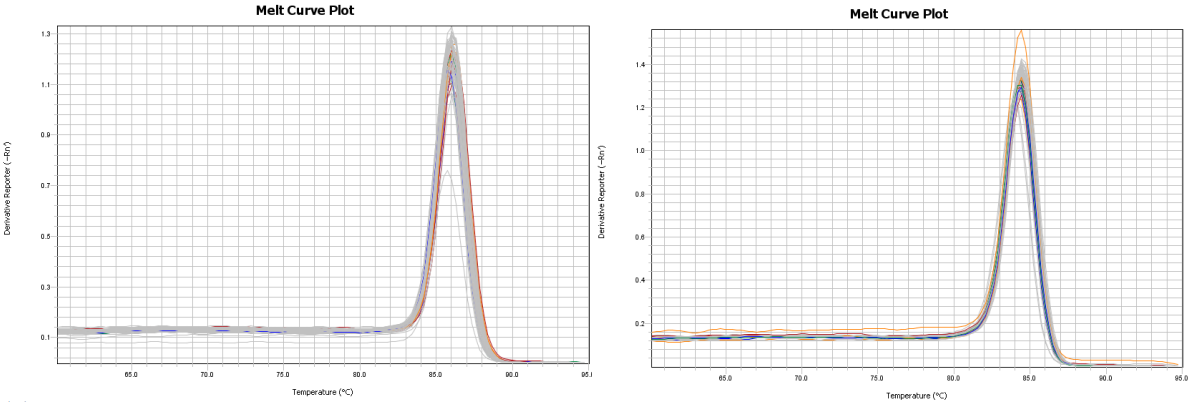

Figure 23. Melt curves of the qPCR of GAPDH (left) and b-actin (right)

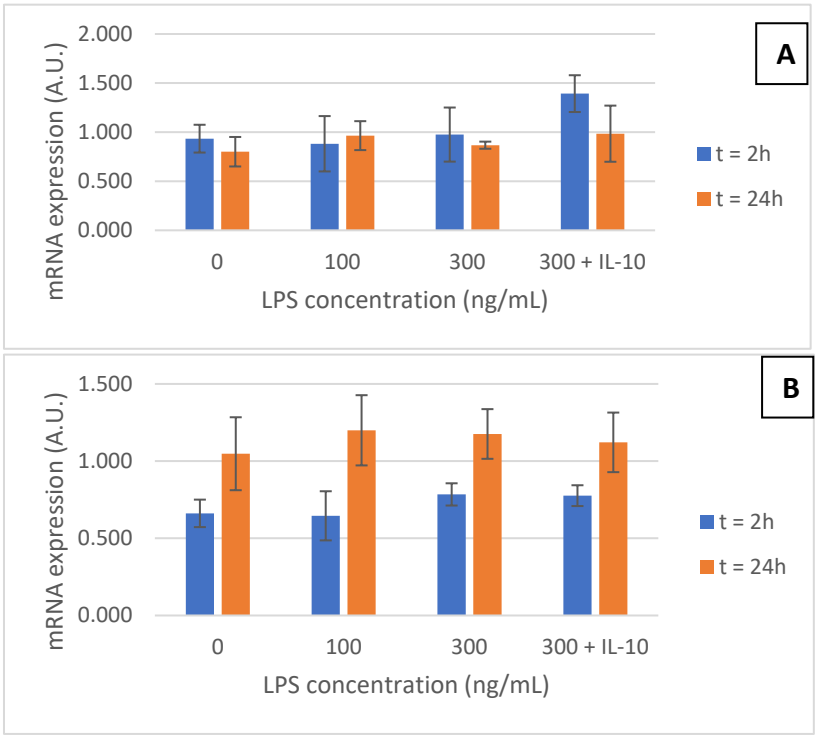

Figure 24. Effect LPS on relative mRNA expression (A) b-actin and (B) GAPDH

Table 7. Data of the GAPDH qPCR corresponding to figure 24

LPS concentration (ng/mL)	***mRNA expression (A.U.)***						***Average concentration (uM) ± SD***
t = 2h	**1**	**2**	**3**	**4**	**5**	**6**	
0	0,82	0,66	0,65	0,62	0,65	0,56	0,66 ± *0,09*
100	0,84	0,71	0,76	0,65	0,51	0,41	0,65 ± *0,16*
300	0,20	0,15	0,12	0,87	0,76	0,73	0,78 ± *0,07*
300 + IL-10	0,88	0,77	0,74	0,83	0,75	0,70	0,78 ± *0,07*
LPS concentration (ng/mL)	***mRNA expression (A.U.)***						***Average concentration (uM) ± SD***
t = 24h	**1**	**2**	**3**	**4**	**5**	**6**	
0	1,46	1,13	0,85	1,10	0,82	0,94	1,05 ± *0,24*
100	1,59	1,12	1,14	1,26	1,18	0,90	1,20 ± *0,23*
300	1,41	1,10	1,11	1,25	0,95	1,25	1,18 ± *0,16*
300 + IL-10	1,23	0,91	0,91	1,41	1,11	1,16	1,12 ± *0,19*

Table 8. Data of the b-actin qPCR corresponding to figure 24

LPS concentration (ng/mL)	***mRNA expression (A.U.)***						***Average concentration (uM) ± SD***
t = 2h	**1**	**2**	**3**	**4**	**5**	**6**	
0	0,95	0,94	1,07	0,77	1,10	0,77	0,93 ± *0,14*
100	1,02	0,96	1,30	0,75	0,80	0,47	0,88 ± *0,28*
300	0,70	0,99	0,65	1,32	0,93	1,26	0,98 ± *0,28*
300 + IL-10	1,36	1,20	1,72	1,49	1,25	1,34	1,39 ± *0,19*
LPS concentration (ng/mL)	***mRNA expression (A.U.)***						***Average concentration (uM) ± SD***
t = 24h	**1**	**2**	**3**	**4**	**5**	**6**	
0	0,97	0,81	0,65	1,01	0,78	0,59	0,80 ± *0,15*
100	1,13	0,96	1,15	0,91	0,93	0,71	0,96 ± *0,15*
300	0,83	0,89	0,83	0,89	0,84	0,93	0,87 ± *0,04*
300 + IL-10	0,92	1,61	0,76	0,82	0,91	0,89	0,98 ± *0,29*

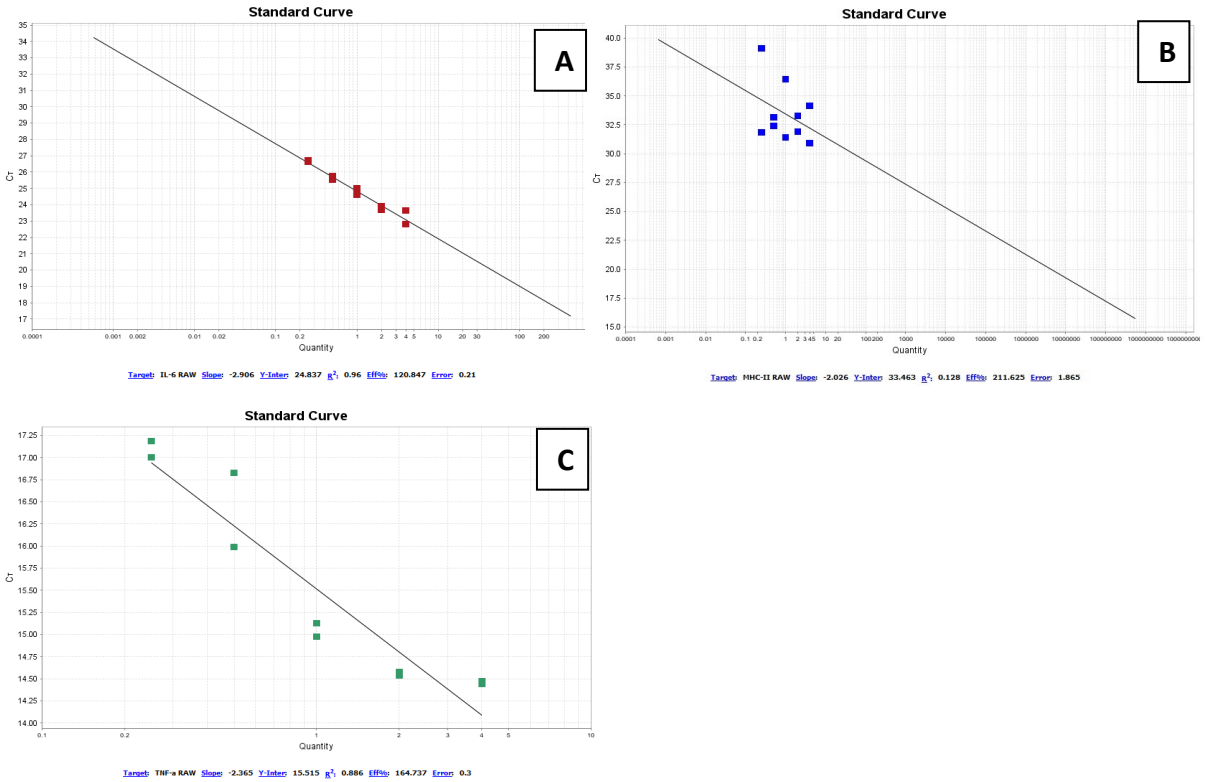

Figure 25. Standard curves of (A) IL-6 (y = -2,906x + 24,837) with an R^2 of 0,96 and an efficiency% of 120,847%, (B) MHC-II (y = -2,026x + 33,463) with an R^2 of 0,128 and an efficiency% of 211,625% and (C) TNF-a (y = -2,365x + 15,515) with an R^2 of 0,886 and an efficiency% of 164,737%

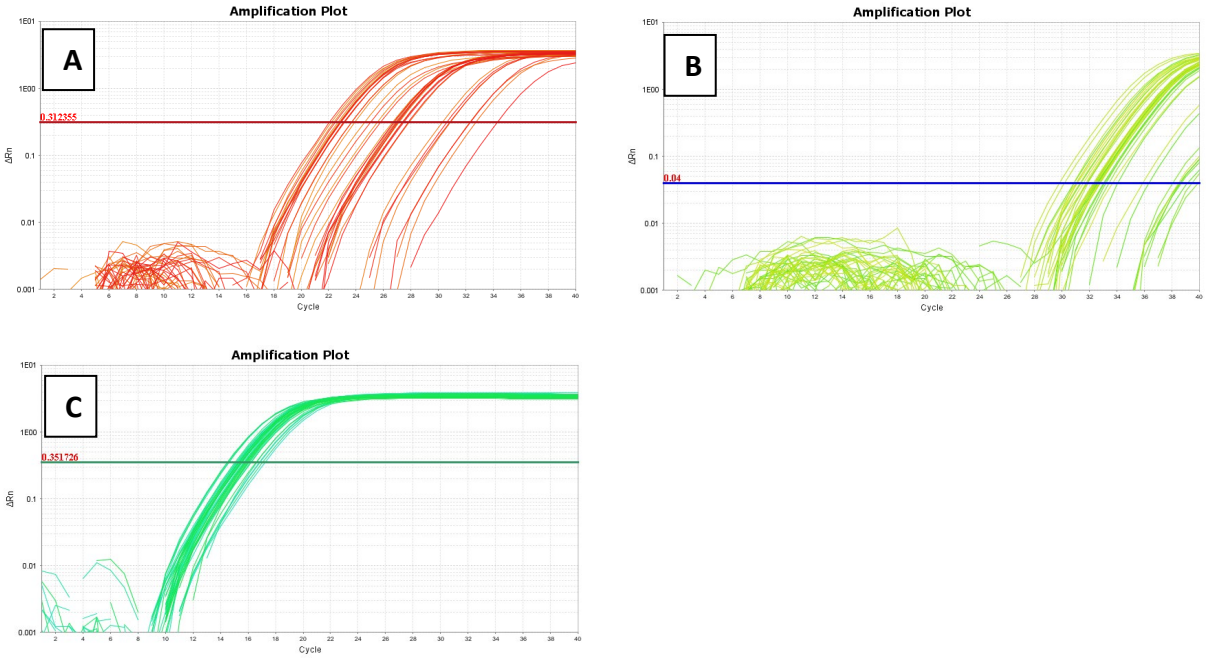

Figure 26. Amplification plots of (A) IL-6, (B) MHC-II and (C) TNF-a

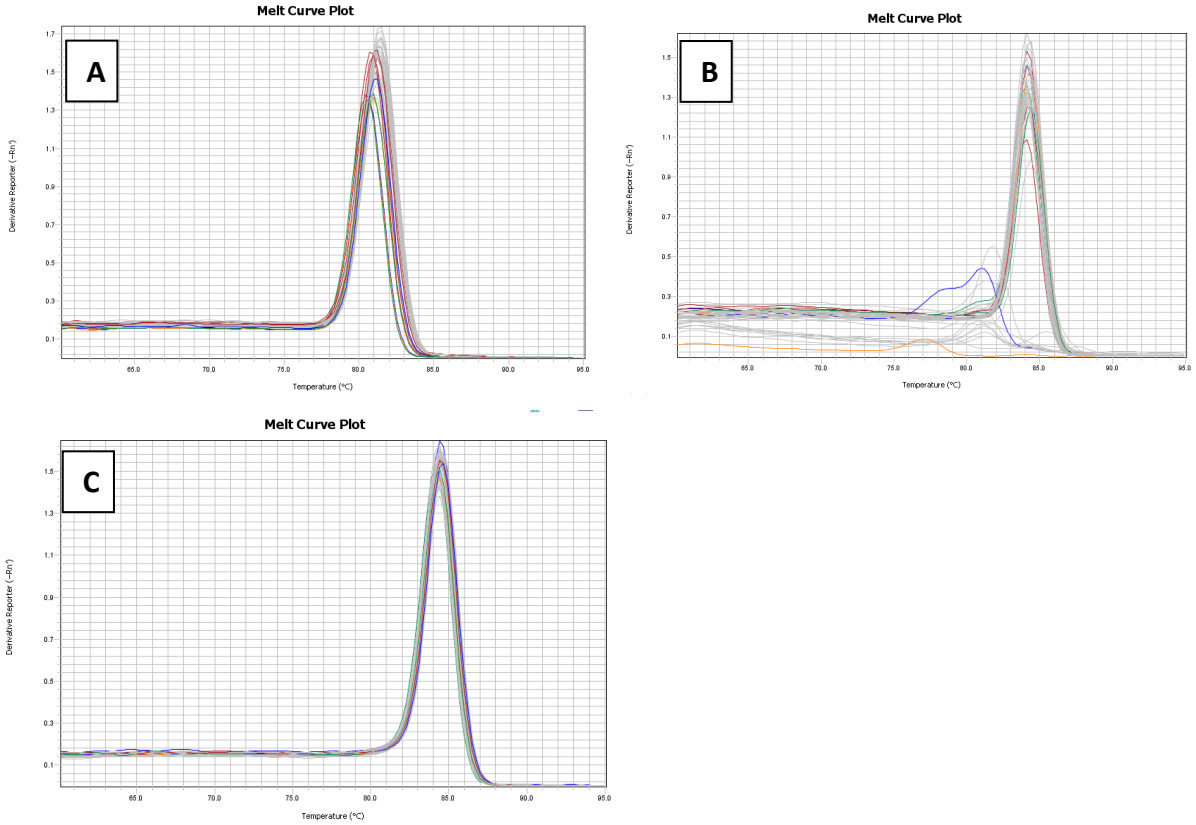

Figure 27. Melt curves of (A) IL-6, (B) MHC-II and (C) TNF-α

Table 9. Data of qPCR of IL-6 corresponding to figure 9

LPS concentration (ng/mL)	***Ct***				***mRNA expression (A.U.)***				***Average mRNA expression (A.U.) ± SD***
t = 2h	**1**	**2**	**3**	**4**	**1**	**2**	**3**	**4**	
0	32,3	32,7	34,3	32,3	0,003	0,002	0,001	0,003	0,00 ± *0,00*
100	27,8	27,9	27,0	27,0	0,096	0,090	0,186	0,184	0,14 ± *0,05*
300	27,5	27,1	27,4	27,4	0,124	0,163	0,132	0,135	0,14 ± *0,02*
300 + IL-10	27,1	27,0	26,8	26,9	0,172	0,174	0,217	0,201	0,19 ± *0,02*
LPS concentration (ng/mL)	***Ct***				***mRNA expression (A.U.)***				***Average mRNA expression (A.U.) ± SD***
t = 24h	**1**	**2**	**3**	**4**	**1**	**2**	**3**	**4**	
0	30,8	30,3	30,6	30,9	0,009	0,014	0,01	0,008	0,01 ± *0,00*
100	23,1	22,7	22,9	22,9	3,977	5,508	4,586	4,667	4,68 ± *0,63*
300	22,1	22,2	22,5	22,4	9,018	8,15	6,348	6,965	7,62 ± *1,19*
300 + IL-10	22,9	22,8	23,2	23,1	4,795	5,07	3,724	3,865	4,36 ± *0,67*

Table 10. Data of qPCR of MHC-II corresponding to figure 9

LPS concentration (ng/mL)	***Ct***				***mRNA expression (A.U.)***				***Average mRNA expression (A.U.) ± SD***
t = 2h	**1**	**2**	**3**	**4**	**1**	**2**	**3**	**4**	
0	32,6	39,9	31,2	39,4	2,821	0,001	13,073	0,001	0,94 ± *1,63*
100	32,8	33,2	31,6	33,5	2,07	1,304	7,998	0,973	3,09 ± *3,31*
300	31,3	31,9	33,7	38,1	12,089	6,123	0,726	0,005	4,74 ± *5,61*
300 + IL-10	32,7	31,5	31,8	32,7	2,291	9,569	6,627	2,505	5,25 ± *3,50*
LPS concentration (ng/mL)	***Ct***				***mRNA expression (A.U.)***				***Average mRNA expression (A.U.) ± SD***
t = 24h	**1**	**2**	**3**	**4**	**1**	**2**	**3**	**4**	
0	32,4	38,6	38,4	38,5	3,367	0,003	0,004	0,003	0,00 ± *0,00*
100	30,3	32,6	35,9	32,8	37,352	2,57	0,062	2,083	1,57 ± *1,33*
300	29,9	38,5	32,8	32,5	59,973	0,003	2,219	2,902	2,56 ± *0,48*
300 + IL-10	31,1	30,9	32,5	32,7	14,052	18,402	3,04	2,426	2,73 ± *0,43*

Table 11. Data of qPCR of TNF-a corresponding to figure 9

LPS concentration (ng/mL)	***Ct***				***mRNA expression (A.U.)***				***Average mRNA expression (A.U.) ± SD***
t = 2h	**1**	**2**	**3**	**4**	**1**	**2**	**3**	**4**	
0	15,9	15,4	16,0	16,6	0,66	1,082	0,653	0,355	0,69 ± *0,30*
100	16,1	15,4	15,3	15,2	0,547	1,138	1,279	1,334	1,07 ± *0,36*
300	15,7	15,4	16,5	16,7	0,805	1,099	0,373	0,289	0,64 ± *0,38*
300 + IL-10	15,3	15,2	15,4	15,1	1,258	1,426	1,078	1,549	1,33 ± *0,20*
LPS concentration (ng/mL)	***Ct***				***mRNA expression (A.U.)***				***Average mRNA expression (A.U.) ± SD***
t = 24h	**1**	**2**	**3**	**4**	**1**	**2**	**3**	**4**	
0	15,9	16,2	15,3	15,3	0,695	0,531	1,238	1,176	0,91 ± *0,35*
100	15,5	15,5	15,5	15,3	1,014	1,012	0,993	1,223	1,06 ± *0,11*
300	15,5	15,7	15,8	15,4	1,063	0,838	0,743	1,078	0,93 ± *0,17*
300 + IL-10	15,7	15,6	15,8	16,1	0,82	0,886	0,748	0,594	0,76 ± *0,13*

Appendix C. Protocols

Protocol NO assay

1. Seed RAW 254.7 cells in a 96-well flat bottom culture plate (100.000 cells in 200 µl/well) in DMEM supplemented with 10% FBS.
2. After 24h, remove supernatant. Add fresh medium containing the following treatment.
   a. Control
   b. LPS 25 ng/ml
   e. LPS 100 ng/ml
3. After 24h incubation, collect 100 ul of the supernatant to measure NO_2^- (one of the end products of NO synthesis)

NO assay:

Materials:

- 100 mM NaNO2 stock solution
- 96 well plate
- 1,5 ml tubes for the standard curve
- Medium of the cells
- Griess solutions:
  - Griess A and Griess B

Calibration curve of Sodium Nitrite ($NaNO_2$):

1. Prepare stock-solution: 100 mM $NaNO_2$-solution in MQ (0.69 g/100 ml) *(Store stock-solution in vials at -20°C)*
2. Dilute stock-solution 100x in culture medium (= 1 mM solution). Pipet 100 ul 100 mM NaNO2 in 10 ml medium ➔1 mM NaNO2 ← stock
3. Make the standard curve:

	NaNO2 uM	V NaNO2 (ul)	V medium (ul)
✓	100	100 ul 1 mM	900 ul
✓	50	500 ul 100 uM	500 ul
✓	25	500 ul 50 uM	500 ul
✓	12.5	500 ul 25 uM	500 ul
✓	6.3	500 ul 12,5 uM	500 ul
✓	3.1	500 ul 6.3 uM	500 ul
✓	1.6	500 ul 3,1 uM	500 ul
X	0.8	500 ul 1,6 uM	500 ul
✓	0	-	500 ul

niet gebruikt

The reaction:

1. Pipet 100 ul of the standard curve samples in triplo in a 96 well plate
2. Pipet 100 ul of your experimental samples in empty wells
3. Make fresh Griess reagent bij mixing equal volume of Griess A and Griess B
4. Pipet 100 ul of this fresh prepared Griess to all the standards and samples
5. Remove the bubbles out of the wells (they disturb the readout)
6. Measure the plate at 550 nM

Figure 28. Protocol used for the NO assay

Promega QuickPROTOCOL 1

Maxwell® 16 LEV simplyRNA Cells Kit

INSTRUCTIONS FOR USE OF PRODUCTS AS1270 AND AS1280.

Preparation of Cell Samples for RNA Purification

Materials to Be Supplied by the User

- centrifuge
- vortex mixer
- RNase-free, sterile, aerosol-resistant pipette tips

Adherent cells:

Wash the monolayer twice with PBS, take off all the medium and store the adherent cells in the plate as soon as possible at -80 until the RNA isolation can be done.

1. Add **200µl** of **chilled 1-Thioglycerol/Homogenization Solution** to the cells and dispense until the cells appear lysed. A pipette may be used to disperse the pellets before vortexting. Store lysed cells on ice if there is a delay before processing.
2. Shortly before processing samples on the Maxwell® 16 Instrument, add **200µl of Lysis Buffer** (Part# MC501C) to the 200µl of lysed cells (from step 1).

   Vortex vigorously for 15 seconds to mix.

   Transfer all 400µl of lysate to well #1 of the Maxwell® 16 LEV Cartridge (MCE). Well #1 is the closest to the cartridge label and farthest from the elution tube.
3. Add 5µl of DNase I solution to well #4 (yellow reagent). After adding the blue DNase I solution, the reagent in well #4 will be green.

Preparation of Tissue Samples for RNA Purification

Materials to Be Supplied by the User

- small tissue homogenizer
- vortex mixer
- tube for homogenization
- RNase-free, sterile, aerosol-resistant pipette tips
- optional: heat block or water bath set to 70°C

1. Homogenize the tissue sample in the chilled 1-Thioglycerol/ Homogenization Solution until no visible tissue fragments remain. Homogenize an additional 15–30 seconds for complete homogenization. If foaming occurs, let sample settle on ice. The final volume of the homogenate added to the cartridge should be 200µl. Add additional homogenization solution as needed to bring samples to a final volume of 200µl.
2. Optional: RNA yield from larger amounts of some tissues may be increased by heating homogenates at 70°C for 2 minutes, then allowing homogenates to cool (approximately 1 minute) before proceeding to Step 3. This is recommended for 10mg or more of liver tissue.

   Note: If the heat step is used, the purified RNA will migrate differently on native gels. Denaturing gels are recommended if the heating step is used.
3. Shortly before processing samples on the Maxwell® 16 Instrument, add 200µl of Lysis Buffer (Part# MC501C) to 200µl of homogenate. Vortex vigorously for 15 seconds to mix. Transfer 400µl to well 1 of the Maxwell® 16 LEV Cartridge (MCE).
4. Add 5µl of DNase to well #4 (yellow reagent). When using more than 5mg of tissues with high DNA content (e.g., liver or spleen), add 10µl of DNase to well #4. After the blue DNase I solution is added, the reagent in well #4 will be green.

Printed in USA. Revised 3/14. Part# 9FB128

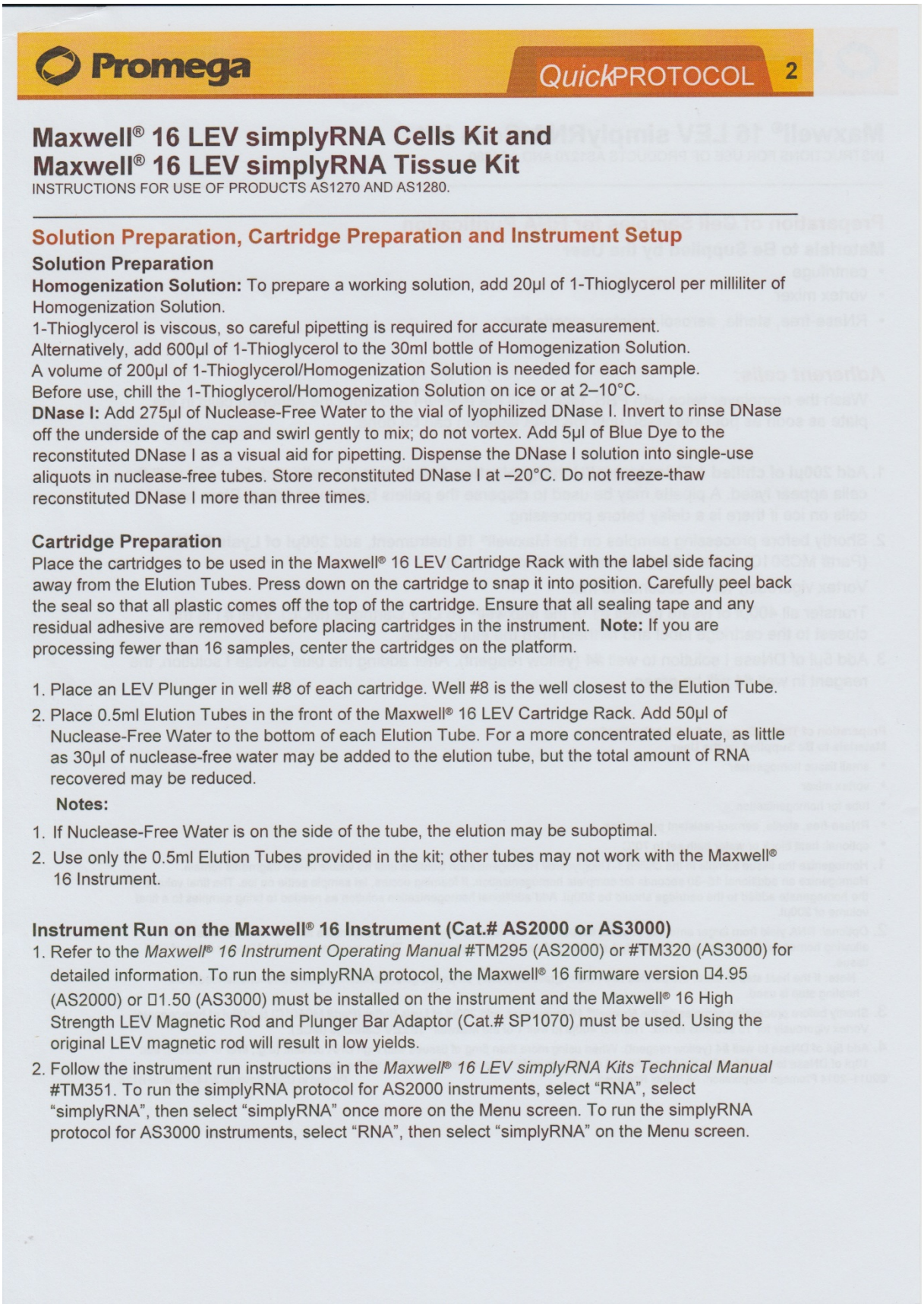

Promega QuickPROTOCOL 2

Maxwell® 16 LEV simplyRNA Cells Kit and Maxwell® 16 LEV simplyRNA Tissue Kit

INSTRUCTIONS FOR USE OF PRODUCTS AS1270 AND AS1280.

Solution Preparation, Cartridge Preparation and Instrument Setup

Solution Preparation

Homogenization Solution: To prepare a working solution, add 20µl of 1-Thioglycerol per milliliter of Homogenization Solution.
1-Thioglycerol is viscous, so careful pipetting is required for accurate measurement.
Alternatively, add 600µl of 1-Thioglycerol to the 30ml bottle of Homogenization Solution.
A volume of 200µl of 1-Thioglycerol/Homogenization Solution is needed for each sample.
Before use, chill the 1-Thioglycerol/Homogenization Solution on ice or at 2–10°C.
DNase I: Add 275µl of Nuclease-Free Water to the vial of lyophilized DNase I. Invert to rinse DNase off the underside of the cap and swirl gently to mix; do not vortex. Add 5µl of Blue Dye to the reconstituted DNase I as a visual aid for pipetting. Dispense the DNase I solution into single-use aliquots in nuclease-free tubes. Store reconstituted DNase I at –20°C. Do not freeze-thaw reconstituted DNase I more than three times.

Cartridge Preparation

Place the cartridges to be used in the Maxwell® 16 LEV Cartridge Rack with the label side facing away from the Elution Tubes. Press down on the cartridge to snap it into position. Carefully peel back the seal so that all plastic comes off the top of the cartridge. Ensure that all sealing tape and any residual adhesive are removed before placing cartridges in the instrument. **Note:** If you are processing fewer than 16 samples, center the cartridges on the platform.

1. Place an LEV Plunger in well #8 of each cartridge. Well #8 is the well closest to the Elution Tube.
2. Place 0.5ml Elution Tubes in the front of the Maxwell® 16 LEV Cartridge Rack. Add 50µl of Nuclease-Free Water to the bottom of each Elution Tube. For a more concentrated eluate, as little as 30µl of nuclease-free water may be added to the elution tube, but the total amount of RNA recovered may be reduced.

Notes:

1. If Nuclease-Free Water is on the side of the tube, the elution may be suboptimal.
2. Use only the 0.5ml Elution Tubes provided in the kit; other tubes may not work with the Maxwell® 16 Instrument.

Instrument Run on the Maxwell® 16 Instrument (Cat.# AS2000 or AS3000)

1. Refer to the *Maxwell® 16 Instrument Operating Manual* #TM295 (AS2000) or #TM320 (AS3000) for detailed information. To run the simplyRNA protocol, the Maxwell® 16 firmware version □4.95 (AS2000) or □1.50 (AS3000) must be installed on the instrument and the Maxwell® 16 High Strength LEV Magnetic Rod and Plunger Bar Adaptor (Cat.# SP1070) must be used. Using the original LEV magnetic rod will result in low yields.
2. Follow the instrument run instructions in the *Maxwell® 16 LEV simplyRNA Kits Technical Manual* #TM351. To run the simplyRNA protocol for AS2000 instruments, select “RNA”, select “simplyRNA”, then select “simplyRNA” once more on the Menu screen. To run the simplyRNA protocol for AS3000 instruments, select “RNA”, then select “simplyRNA” on the Menu screen.

Figure 29. Protocols used for the the RNA isolation and conversion to cDNA

Real Time PCR with Absolute QPCR

Reservation of the CFX machine:
www.internetagenda.nl
inlognaam: rtpcr
wachtwoord KFF

Note: For the Biorad CFX 384 you need 10 ul total volume for the PCR (Pipet with electronic repeating pipet for extra accuracy).

1. **Prepare cDNA for the standard curve**: 10 ul of cDNA of the 12 random samples.

Standard curve	cDNA mix all samples	Add RNAse free water
4	120 ul total (sum of the 12 samples)	180 ul
2	120 ul of 4x	120 ul
1	120 ul of 2x	120 ul
0,5	120 ul of 1x	120 ul
0,25	120 ul of 0,5x	120 ul
Neg Control	-	120 ul

2. **Prepare your primer-stocks** final concentration 50 uM.
3. **Prepare your primer-mix** of 10 uM
   a. 20 ul forward primer + 20 ul reverse primer + 60 ul RNAse free water.
4. **Dilute your cDNA samples**: 10 ul of cDNA + 90 ul of H2O.
5. **Prepare the PCR master mix *per primer*,**
   note for each primer set you use, also include a standard curve for that primer set!

Example; 12 normal samples, 6 standard curve samples, 2 primers to be used (HSPA1A and housekeeping GAPDH);
total amount of samples for PCR master mix;

Primer 1: (total 60)
12 samples in triplo 36
6 standard curve in triplo 18
54 + 6 extra (10% pipeting error)

Primer 2: (total 60)
12 samples in triplo 36
6 standard curve in triplo 18
54 + 6 extra (10% pipeting error)

PCR master mix per sample:

sybergreen ROX mix	5.0 ul	x 150 =	750 µl	210 µl
Primer F + R (10 uM)	0.3 ul	x 150 =	450 µl	15 µl
H2O	2.7 ul	x 150 =	405 µl	135 µl
	Vt = 8.0 ul		1200 µl	400 µl

per gene

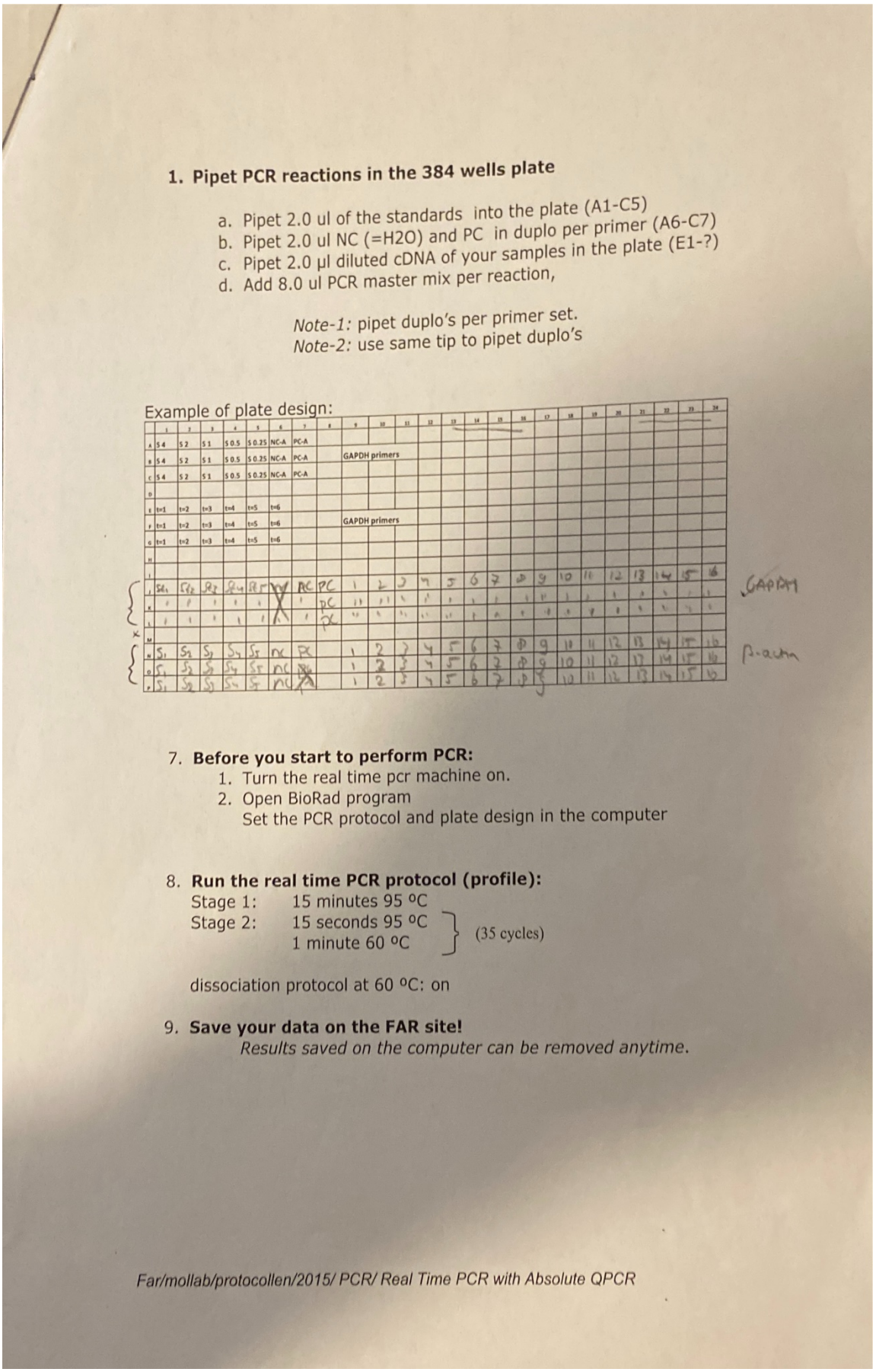

1. **Pipet PCR reactions in the 384 wells plate**

   a. Pipet 2.0 ul of the standards into the plate (A1-C5)
   b. Pipet 2.0 ul NC (=H2O) and PC in duplo per primer (A6-C7)
   c. Pipet 2.0 µl diluted cDNA of your samples in the plate (E1-?)
   d. Add 8.0 ul PCR master mix per reaction,

   Note-1: pipet duplo's per primer set.
   Note-2: use same tip to pipet duplo's

Example of plate design:

	1	2	3	4	5	6	7	8	9	10	11	12	13	14	15	16	17	18	19	20	21	22	23	24
A	S4	S2	S1	S0.5	S0.25	NC-A	PC-A																	
B	S4	S2	S1	S0.5	S0.25	NC-A	PC-A		GAPDH primers															
C	S4	S2	S1	S0.5	S0.25	NC-A	PC-A																	
D																								
E	t=1	t=2	t=3	t=4	t=5	t=6																		
F	t=1	t=2	t=3	t=4	t=5	t=6			GAPDH primers															
G	t=1	t=2	t=3	t=4	t=5	t=6																		
H																								
I																								
J	S1	S2	S3	S4	S5	NC	PC		1	2	3	4	5	6	7	8	9	10	11	12	13	14	15	16
K							PC																	
L							PC																	
M																								
N	S1	S2	S3	S4	S5	NC	PC		1	2	3	4	5	6	7	8	9	10	11	12	13	14	15	16
O	S1	S2	S3	S4	S5	NC	PC		1	2	3	4	5	6	7	8	9	10	11	12	13	14	15	16
P	S1	S2	S3	S4	S5	NC	PC		1	2	3	4	5	6	7	8	9	10	11	12	13	14	15	16

GAPDH

β-actin

7. **Before you start to perform PCR:**
   1. Turn the real time pcr machine on.
   2. Open BioRad program
      Set the PCR protocol and plate design in the computer

8. **Run the real time PCR protocol (profile):**
   Stage 1: 15 minutes 95 °C
   Stage 2: 15 seconds 95 °C
   1 minute 60 °C } (35 cycles)

   dissociation protocol at 60 °C: on

9. **Save your data on the FAR site!**
   Results saved on the computer can be removed anytime.

Far/mollab/protocollen/2015/ PCR/ Real Time PCR with Absolute QPCR

Figure 30. Protocol used for running the qPCR

Immunohistochemical staining with NovaRed

Date:

- Dry sections for 20 minutes with a föhn.
- Fixation with aceton for 10 minutes (max. 15 minutes).
- Dry the sections on the air.
- Draw circle around the sections with a dakopen. (wait till dakopen is dry before further steps)
- Rinse in PBS for 5 minutes (change PBS 3x).

Important: take care that sections do not dry up after this step!

Endogeneous peroxidase blocking:

- Incubate in 0,3% H_2O_2 in 100% methanol (0,6 ml H_2O_2 in 60 ml MeOH) for 20 minutes.
- Rinse with water for 2-3 minutes.
- Rinse in PBS for 5 minutes (change PBS 3x)

- 1st antibody incubation for 60 minutes
- 50µl per section.
- Rinse in PBS for 5 minutes (change PBS 3x).

- 2nd antibody incubation for 30 minutes. Do not forget to put 5% of normal serum (of the species of your sections); 50µl per section.
- Rinse in PBS for 5 minutes (change PBS 3x)

- 3rd antibody incubation for 30 minutes. Do not forget to put 5% of normal serum (of the species of your sections); 50µl per section.
- Rinse in PBS for 5 minutes (change PBS 3x)

- Rinse in aqua dest.

- Staining with NovaRed kit for max 10 minutes
- Wash with dH_2O

- Incubate for 5 minutes in hematoxillin
- Rinse in tap water (10 minutes)
- Dehydrate
- Cover the section with a coverglass using ???

Figure 31. Protol used for the histochemical staining